Group theoretic approach to large-deformation property of three-dimensional bar-hinge mechanism

AUTHOR(S):

Watada, Ryo; Ohsaki, Makoto; Kanno, Yoshihiro

CITATION:

Watada, Ryo ...[et al]. Group theoretic approach to large-deformation property of three-dimensional bar-hinge mechanism. Japan Journal of Industrial and Applied Mathematics 2019, 36(1): 177-208

ISSUE DATE:

2019-01

URL:

http://hdl.handle.net/2433/243153

Submitted to Japan Journal of Industrial and Applied Mathematics manuscript No.
(will be inserted by the editor)

Group theoretic approach to large-deformation property of three-dimensional bar-hinge mechanism

Ryo Watada · Makoto Ohsaki · Yoshihiro Kanno

Received: date / Accepted: date

Abstract A group-theoretic approach is presented for investigation of large-deformation property of bar-hinge mechanisms with dihedral symmetry in three-dimensional space. The number of the compatibility conditions at bar-ends is reduced by formulating them with respect to the null space of the linear compatibility matrix. It is shown that the system of reduced compatibility equations inherits the group equivariance from the original compatibility equations. This inheritance is used to develop a method to judge whether the frame has a finite mechanism mode. Sufficient conditions for large deformation mechanisms are derived based on the symmetry properties of infinitesimal mechanism modes and generalized self-equilibrium force modes. The detailed procedure of the method is shown through the numerical examples.

Keywords bar-joint mechanism · artibtrarily inclined hinge · group theory · dihedral group

1 Introduction

Group theory has been used for modeling symmetry properties in various fields of engineering [1]. Ikeda and Murota [2] presented a group-theoretic approach

R. Watada
Department of Architecture and Architectural Engineering, Kyoto University, Kyoto-Daigaku Katsura, Nishikyo, Kyoto 615-8540, Japan
Takenaka Corporation, 4-1-13, Hommachi, Chuo, Osaka 541-0053, Japan
E-mail: se.watada@archi.kyoto-u.ac.jp

M. Ohsaki
Department of Architecture and Architectural Engineering, Kyoto University, Japan
E-mail: ohsaki@archi.kyoto-u.ac.jp

Y. Kanno
Mathematics and Informatics Center, The University of Tokyo, Japan
E-mail: kanno@mist.i.u-tokyo.ac.jp

to investigation of buckling behaviors of symmetric structures. Ikeda *et al.* [3] proposed a method of imperfection sensitivity analysis of a structure with dihedral symmetry exhibiting hilltop branching that has a bifurcation point at a limit point. Zhang *et al.* [4] investigated equilibrium and stability of a tensegrity structure with dihedral symmetry. Kanno *et al.* [5] studied semidefinite programming problems whose data have group-symmetry properties. Cen and Feng [6] investigated the symmetry of eigenmodes of prestressed structures using block-diagonalized forms of the stiffness and mass matrices.

Linkage mechanism, as shown in Fig. 1 is defined as a structure that can have deformation without application of external loads. Such structure consists of linkages connected by joints or hinges. In this paper, we consider frame models consisting of bars connected by revolute joints and universal joints. Ohsaki *et al.* [7] proposed an optimization-based approach for generating frame mechanisms, where a linear programming problem is solved to obtain an infinitesimal mechanism of a bar-hinge structure. The approach has been extended to incorporate hinges in arbitrary directions, which is obtained by solving a quadratic programming problem [8].

A mechanism is said to be an infinitesimal mechanism if deformation without force is allowed only if the deformation is sufficiently small; otherwise, it is called a finite mechanism. Guest and Fowler [9] showed that a mechanism is finite if it has no self-equilibrium force, or the self-equilibrium forces are in a different symmetry property from the deformation mode. Schulze et al. [10]

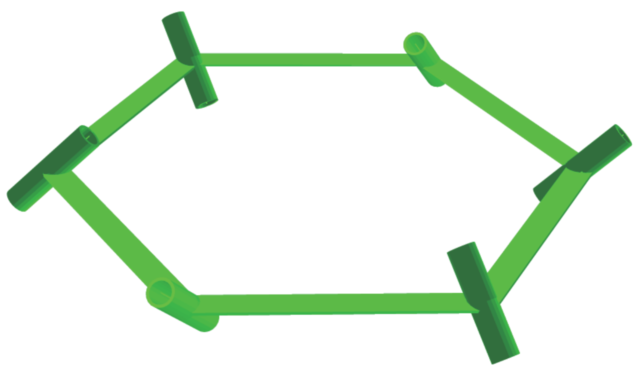

Fig. 1 An example of linkage. Six bars are connected by six revolute joints (hinges) to form a hexagonal bar-hinge mechanism.

investigated necessary conditions for simultaneously statically and kinematically indeterminate body-hinge structure using characters of group theory. Watada and Ohsaki [11] proposed a series expansion method for evaluating the order of mechanism.

Ikeshita [12] applied the group-theoretic bifurcation theory [2] to the pin-jointed bar structures with symmetric configurations. He studied two cases: (i) a structure with one degree of kinematical indeterminacy and one degree of statical indeterminacy, and (ii) a statically determinate structure with one degree of kinematical indeterminacy. Concerning the bifurcation point on the deformation path of a symmetric mechanism, he showed that the symmetry of the bifurcated path is represented by a subgroup of the group representing the symmetry of the configuration of the mechanism at the bifurcation point. Also, from the group equivariance of the compatibility equation, he derived sufficient conditions for a structure with one degree of kinematical indeterminacy and one degree of statical indeterminacy to have a finite mechanism. However, his study focuses on only pin-jointed structures. Moreover, the case in which the degree of internal statical indeterminacy is greater than one is not considered.

In this paper, we consider a three-dimensional bar-hinge mechanism which has dihedral symmetry. The compatibility conditions at the bar-ends are reduced to those with respect to the null space of the linear compatibility matrix. Symmetry conditions are expressed using the irreducible representations of dihedral symmetry. Sufficient conditions for large deformation mechanism are derived based on the symmetry conditions of mechanism modes and generalized self-equilibrium force modes. The conditions are verified in the numerical examples.

In our notation, we use $\dim(\cdot)$, $\mathrm{rank}(\cdot)$, $\ker(\cdot)$, $\mathrm{range}(\cdot)$ and $\mathrm{span}(\cdot)$ to denote the dimension of a linear space, the rank of a matrix, the kernel space of a matrix, the range space of a matrix and the span of a vector space, respectively.

2 Group equivariance of compatibility relations

2.1 Compatibility between generalized displacements and strains

Consider a three-dimensional bar-hinge mechanism consisting of bars connected by revolute joints, which are called *hinges* for brevity. The mechanism can also have a universal joint that can rotate along two axes. A deformed shape of the mechanism is defined by the *generalized displacement vector* $\boldsymbol{W} \in \mathbb{R}^f$ consisting of displacements and rotations of nodes and bars, where f is the total number of degrees of freedom. A system of compatibility equations of the bar-hinge mechanism is described as follows:

$$\boldsymbol{C}(\boldsymbol{W}) = \boldsymbol{0}, \tag{1}$$

where $\boldsymbol{C}(\boldsymbol{W}) \in \mathbb{R}^m$ is called *incompatibility vector*, which is a vector of incompatibility of displacements and rotations at two ends of each bar. Here m denotes the number of components of $\boldsymbol{C}(\boldsymbol{W})$.

There are several ways of describing compatibility of mechanism exhibiting finite displacement and rotation. In this paper, finite rotation is expressed using the Euler parameter [13,14]. The translation vector of node k and the center of bar i with respect to the global coordinate system (x_1, x_2, x_3) are denoted by $\boldsymbol{U}_k = (U_k^1, U_k^2, U_k^3)^\top$ and $\boldsymbol{V}_i = (V_i^1, V_i^2, V_i^3)^\top$, respectively. The rotation vector of node k and the center of bar i around global axes are denoted by $\boldsymbol{\Theta}_k = (\Theta_k^1, \Theta_k^2, \Theta_k^3)^\top$ and $\boldsymbol{\Psi}_i = (\Psi_i^1, \Psi_i^2, \Psi_i^3)^\top$, respectively, each of which defines the axis of rotation and its norm corresponds to the amount of rotation. The generalized displacement vector $\boldsymbol{W}$ is composed of $\boldsymbol{U}$, $\boldsymbol{\Theta}$, $\boldsymbol{V}$ and $\boldsymbol{\Psi}$. The detailed derivation of the incompatibility vector $\boldsymbol{C}(\boldsymbol{W})$ used in this paper is described in Ref. [11], which is summarized in Appendix A. 1.

2.2 Group equivariance of compatibility relations

Suppose the frame has geometrical symmetry, which is expressed using group representation. Let G denote the group of geometrical transformations g which retain the frame configuration invariant. In this paper, we study dihedral symmetry $G = \mathrm{D}_n$. In this section, the group equivariance of the compatibility equation is investigated for the frame that has geometrical symmetry represented as group G.

The symmetry of compatibility equations (1) has the following *equivariance* to a group G:

$$S(g)\boldsymbol{C}(\boldsymbol{W}) = \boldsymbol{C}(T(g)\boldsymbol{W}), \quad g \in G, \tag{2}$$

where $S(g)$ is a unitary matrix representation of $g \in G$ in the m-dimensional space expressing the transformation of incompatibility vector by action g. Similarly, $T(g)$ is a unitary matrix representation of g in the f-dimensional space of generalized displacement vector. Eq. (2) implies that if $\boldsymbol{W}$ satisfies (1), then $T(g)\boldsymbol{W}$ also satisfies $\boldsymbol{C}(T(g)\boldsymbol{W}) = \boldsymbol{0}$ for any $g \in G$.

Let $\Gamma(\boldsymbol{W}) \in \mathbb{R}^{m\times f}$ denote the linear compatibility matrix. Its (s,i) component, denoted by $\Gamma_{si}(\boldsymbol{W})$, is defined as

$$\Gamma_{si}(\boldsymbol{W}) = \frac{\partial C_s(\boldsymbol{W})}{\partial W_i}. \tag{3}$$

Then, differentiating (2) with respect to $\boldsymbol{W}$, we obtain

$$S(g)\Gamma(\boldsymbol{W}) = \Gamma(T(g)\boldsymbol{W})T(g), \quad g \in G. \tag{4}$$

Eq. (4) describes the *equivariance of the compatibility matrix* to G.

2.3 Reduction of compatibility equation

In this section, the number of the equations of the equivariance of the compatibility matrix expressed as (4) is reduced using the methodology based on Ikeda and Murota [2]. They derived the group equivariance of a system of nonlinear equiribrium equations. We basically follow the method they proposed and apply it to the system of the compatibility matrix (4) with two matrix representations $S(g)$ and $T(g)$.

In the following, the *Liapunov–Schmidt reduction procedure* [2,15,16] is used to reduce the number of compatibility equations. Let $\varGamma_* := \varGamma(\mathbf{0})$ denote the compatibility matrix at the undeformed state $\boldsymbol{W} = \mathbf{0}$.

Define p, q and u as

$$p := \dim[\ker(\varGamma_*)] = f - u, \tag{5a}$$
$$q := \dim[\ker(\varGamma_*^\top)] = m - u, \tag{5b}$$
$$u := \operatorname{rank}(\varGamma_*) = \operatorname{rank}(\varGamma_*^\top). \tag{5c}$$

Consider a direct sum decomposition of the spaces $\mathbb{R}^f$ and $\mathbb{R}^m$ of $\boldsymbol{W} \in \mathbb{R}^f$ and $\boldsymbol{C}(\boldsymbol{W}) \in \mathbb{R}^m$, respectively, as [18]

$$\mathbb{R}^f = \ker(\varGamma_*) \oplus U, \tag{6a}$$
$$\mathbb{R}^m = V \oplus \operatorname{range}(\varGamma_*). \tag{6b}$$

Though the subspaces U and V are not determined uniquely, we make a natural choice of them as

$$U = \operatorname{range}(\varGamma_*^\top), \quad V = \ker(\varGamma_*^\top). \tag{7}$$

We take an orthonormal basis $\{\boldsymbol{\eta}_i \mid i = 1, \ldots, f\}$ of $\mathbb{R}^f$ such that $\{\boldsymbol{\eta}_i \mid i = 1, \ldots, p\}$ is a basis of $\ker(\varGamma_*)$ and $\{\boldsymbol{\eta}_i \mid i = p+1, \ldots, f\}$ is a basis of U. Also, we take an orthonormal basis $\{\boldsymbol{\zeta}_i \mid i = 1, \ldots, m\}$ of $\mathbb{R}^m$ such that $\{\boldsymbol{\zeta}_i \mid i = 1, \ldots, q\}$ is a basis of V and $\{\boldsymbol{\zeta}_i \mid i = q+1, \ldots, m\}$ is a basis of $\operatorname{range}(\varGamma_*)$. Note that $\boldsymbol{\eta}_1, \ldots, \boldsymbol{\eta}_p$ are *infinitesimal mechanism mode vectors* satisfying $\varGamma_* \boldsymbol{\eta}_i = \mathbf{0}$ $(i = 1, \ldots, p)$. In this paper, we call $\boldsymbol{\zeta}_1, \ldots, \boldsymbol{\zeta}_q$ as *generalized self-equilibrium force mode vectors* because $\varGamma_*^\top$ is regarded as a generalized equilibrium matrix.

The vector $\boldsymbol{W}$ is additively decomposed into two components $\boldsymbol{w} \in \ker(\varGamma_*)$ and $\overline{\boldsymbol{w}} \in U$ as

$$\boldsymbol{W} = \boldsymbol{w} + \overline{\boldsymbol{w}}. \tag{8}$$

Let $P : \mathbb{R}^m \to \mathbb{R}^m$ denote the projection matrix onto V, which is obtained as

$$P = \sum_{i=1}^{q} \boldsymbol{\zeta}_i \boldsymbol{\zeta}_i^\top. \tag{9}$$

Then, (1) is decomposed into the following two equations:

$$P \cdot \boldsymbol{C}(\boldsymbol{w} + \overline{\boldsymbol{w}}) = \mathbf{0}, \tag{10a}$$
$$(I - P) \cdot \boldsymbol{C}(\boldsymbol{w} + \overline{\boldsymbol{w}}) = \mathbf{0}. \tag{10b}$$

The implicit function theorem ensures that (10b) can be solved for $\overline{\boldsymbol{w}}$ uniquely in a neighborhood of $(\boldsymbol{w}, \overline{\boldsymbol{w}}) = (\mathbf{0}, \mathbf{0})$ as

$$\overline{\boldsymbol{w}} = \boldsymbol{\phi}(\boldsymbol{w}), \quad \mathbf{0} = \boldsymbol{\phi}(\mathbf{0}). \tag{11}$$

See [2,15,16] for details. Substituting $\overline{\boldsymbol{w}}$ in (11) into (10a), we obtain the *reduced system of compatibility equations* with respect to $\boldsymbol{w}$ as

$$\tilde{\boldsymbol{C}}(\boldsymbol{w}) := P \cdot \boldsymbol{C}(\boldsymbol{w} + \boldsymbol{\phi}(\boldsymbol{w})) = \mathbf{0}. \tag{12}$$

A p-dimensional vector $\boldsymbol{v} := [v_1, \ldots, v_p]^\top \in \mathbb{R}^p$ is introduced to express $\boldsymbol{w} \in \ker \Gamma_*$ using the infinitesimal mechanism modes $\{\boldsymbol{\eta}_i \mid i = 1, \ldots, p\}$ as follows:

$$\boldsymbol{w} = [\boldsymbol{\eta}_1, \ldots, \boldsymbol{\eta}_p]\boldsymbol{v}. \tag{13}$$

Since $\tilde{\boldsymbol{C}}(\boldsymbol{w})$ of (12) is an m-dimensional vector projected onto q-dimensional subspace V of $\mathbb{R}^m$ with respect to $\boldsymbol{w}$ expressed by $\boldsymbol{v}$, $\tilde{\boldsymbol{C}}(\boldsymbol{w})$ can be expressed, as follows, using a q-dimentional coefficient vector $\hat{\boldsymbol{C}}(\boldsymbol{v}) = [\hat{C}_1(\boldsymbol{v}), \ldots, \hat{C}_q(\boldsymbol{v})]^\top \in \mathbb{R}^q$ for the generalized self-equilibrium force modes $\{\boldsymbol{\zeta}_i \mid i = 1, 2, \ldots, q\}$, which are the basis vectors of V:

$$\tilde{\boldsymbol{C}}(\boldsymbol{w}) = \sum_{i=1}^{q} \hat{C}_i(\boldsymbol{v})\boldsymbol{\zeta}_i = [\boldsymbol{\zeta}_1, \ldots, \boldsymbol{\zeta}_q]\hat{\boldsymbol{C}}(\boldsymbol{v}). \tag{14}$$

Next, the reduction procedure described above is applied to the system of compatibility equations, which has group equivariance shown in (2). The fundamental properties are summarized as follows:

- $\ker(\Gamma_*)$ is G-invariant with respect to $T(g)$, and $\mathrm{range}(\Gamma_*)$ is G-invariant with respect to $S(g)$.
- U and V in (7) can be chosen so as to be G-invariant with respect to $T(g)$ and $S(g)$, respectively.

See Lemma 7.2 of [2] for details. Then, it can be shown that the system of reduced compatibility equations (12) inherits group equivariance (2) from the original compatibility equation (1). In other words, group equivariance of the reduced compatibility (12) is expressed as

$$S(g)\tilde{\boldsymbol{C}}(\boldsymbol{w}) = \tilde{\boldsymbol{C}}(T(g)\boldsymbol{w}), \quad g \in G. \tag{15}$$

Furthermore, using (14), we can reduce (15) to

$$\hat{S}(g)\hat{\boldsymbol{C}}(\boldsymbol{v}) = \hat{\boldsymbol{C}}(\hat{T}(g)\boldsymbol{v}), \quad g \in G, \tag{16}$$

where $\hat{S}(g) \in \mathbb{R}^{q \times q}$ and $\hat{T}(g) \in \mathbb{R}^{p \times p}$ satisfy

$$S(g)[\boldsymbol{\zeta}_1, \ldots, \boldsymbol{\zeta}_q] = [\boldsymbol{\zeta}_1, \ldots, \boldsymbol{\zeta}_q]\hat{S}(g), \quad g \in G, \tag{17a}$$

$$T(g)[\boldsymbol{\eta}_1, \ldots, \boldsymbol{\eta}_p] = [\boldsymbol{\eta}_1, \ldots, \boldsymbol{\eta}_p]\hat{T}(g), \quad g \in G. \tag{17b}$$

See [2,17] for details.

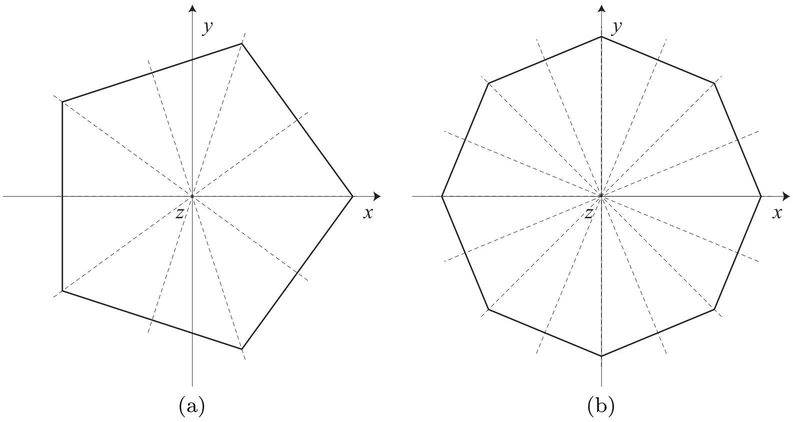

Fig. 2 Examples of dihedral symmetry D_n; (a) D_5, (b) D_8

3 Prediction of large-deformation property of D_n-equivariant system

From the viewpoint of practical application, it is important to judge whether the frame has a finite mechanism mode ensuring that the frame remains unstable along large-deformation. In this section, we show a method to predict the large-deformation property of D_n symmetric system using the reduced compatibility equations (16).

3.1 One dimensional irreducible representation of dihedral group

Dihedral symmetry of nth order D_n represents symmetry properties of a regular n-sided polygon, which has n degrees of rotational symmetry and n axes of reflection symmetry as illustrated in Fig. 2.

Dihedral group D_n is defined as

$$\begin{aligned}\mathrm{D}_n &= \left\{r^i, sr^i \mid i = 0, \ldots, n-1\right\} \\ &= \left\{e, r, \ldots, r^{n-1}, s, sr, \ldots, sr^{n-1}\right\},\end{aligned} \tag{18}$$

where r denotes a counterclockwise rotation around z-axis by an angle $2\pi/n$, s denotes a reflection with respect to xz plane, i.e., $y \mapsto -y$, and e denotes the identity transformation. Here r and s satisfy the following relations:

$$r^i r^j = r^{i+j}, \quad r^n = s^2 = (sr)^2 = e. \tag{19}$$

Consider a D_n symmetric frame that has a single infinitesimal mechanism mode, i.e., $p = f - u = 1$. Initial state of the frame is defined as $\boldsymbol{W} = \boldsymbol{0}$. Note that, in this case, we can define

$$\xi := v_1 \in \mathbb{R} \tag{20}$$

as a *path parameter* representing deformation of the frame. Using a path parameter ξ of (20), (16) is rewritten as

$$\hat{S}(g)\hat{\boldsymbol{C}}(\xi) = \hat{\boldsymbol{C}}(\hat{T}(g)\xi), \tag{21}$$

where $\hat{T}(g)$ is a 1×1 matrix representation of G, and therefore, irreducible. Let ν denote the irreducible representation index. For a D_n-equivariant system, it is known that ν and its one-dimensional representations $T^{\nu}(g)$ are expressed as follows:

$$\nu \in \begin{cases} \{A_1, A_2, B_1, B_2\} & \text{(for } n \text{ even)}, \quad (22a) \\ \{A_1, A_2\} & \text{(for } n \text{ odd)}, \quad (22b) \end{cases}$$

where

$$T^{A_1}(r) = 1, \quad T^{A_1}(s) = 1, \tag{23a}$$
$$T^{A_2}(r) = 1, \quad T^{A_2}(s) = -1, \tag{23b}$$
$$T^{B_1}(r) = -1, \quad T^{B_1}(s) = 1, \tag{23c}$$
$$T^{B_2}(r) = -1, \quad T^{B_2}(s) = -1. \tag{23d}$$

Investigating the property of rotational and reflectional symmetry of $\boldsymbol{\eta}_1$, we can determine which of (23a)–(23d) is satisfied by $T^{\nu}(g)$ for a $g \in \mathrm{D}_n$. Since (17b) holds, $T^{\nu}(g)$ can be calculated from $T(g)$ and $\boldsymbol{\eta}_1$ as

$$T^{\nu}(g) = \boldsymbol{\eta}_1^{\top} T(g) \boldsymbol{\eta}_1, \quad g \in \mathrm{D}_n. \tag{24}$$

In the following, two cases of the number of generalized self-equilibrium force modes, $q = 1$ and $q \geq 2$, are investigated, while p is restricted to 1.

3.2 Finite mechanism with single generalized self-equilibrium force mode

When the number of generalized self-equilibrium force modes is 1, i.e., $q = 1$, (17a) means that $\hat{S}(g)$ is a 1×1 matrix representation of D_n, and therefore irreducible. We write it as $S^{\mu}(g)$ with an irreducible representation index μ.

In a similar manner as (22a), (22b) and (23a)–(23d) for $T^{\nu}(g)$, μ and $S^{\mu}(g)$ are determined as follows:

$$\mu \in \begin{cases} \{A_1, A_2, B_1, B_2\} & \text{(for } n \text{ even)}, \quad (25a) \\ \{A_1, A_2\} & \text{(for } n \text{ odd)}, \quad (25b) \end{cases}$$

where

$$S^{A_1}(r) = 1, \quad S^{A_1}(s) = 1, \tag{26a}$$
$$S^{A_2}(r) = 1, \quad S^{A_2}(s) = -1, \tag{26b}$$
$$S^{B_1}(r) = -1, \quad S^{B_1}(s) = 1, \tag{26c}$$
$$S^{B_2}(r) = -1, \quad S^{B_2}(s) = -1. \tag{26d}$$

$S^\mu(g)$ can be calculated from $S(g)$ and $\boldsymbol{\zeta}_1$, as follows, in the same manner as $T^\nu(g)$:

$$S^\mu(g) = \boldsymbol{\zeta}_1^\top S(g)\boldsymbol{\zeta}_1, \quad g \in \mathrm{D}_n. \tag{27}$$

Finally, (21) is expressed as

$$S^\mu(g)\hat{C}(\xi) = \hat{C}(T^\nu(g)\xi), \quad g \in \mathrm{D}_n. \tag{28}$$

Suppose that there exists an element h of D_n satisfying $T^\nu(h) = 1$ and $S^\mu(h) = -1$. This is the case for the pairs $(\nu, \mu) = (A_1, A_2), (A_1, B_1), (A_1, B_2), (A_2, B_1), (A_2, B_2), (B_1, A_2), (B_1, B_2), (B_2, A_2)$ and (B_2, B_1). Then, the following equation should hold from (28):

$$-\hat{C}(\xi) = \hat{C}(\xi) \;\Leftrightarrow\; \hat{C}(\xi) = 0. \tag{29}$$

This means that $\hat{C}(\xi)$ remains 0 identically for any ξ; accordingly, the frame has a finite mechanism mode.

Combinations of ν and μ for guaranteeing existence of a finite mechanism are summarized as follows:

$$\begin{aligned}(\nu, \mu) \in \{&(A_1, A_2), (A_1, B_1), (A_1, B_2), (A_2, B_1),\\ &(A_2, B_2), (B_1, A_2), (B_1, B_2), (B_2, A_2), (B_2, B_1)\} \quad (\text{for } n \text{ even}),\end{aligned} \tag{30a}$$

$$(\nu, \mu) = (A_1, A_2) \quad (\text{for } n \text{ odd}). \tag{30b}$$

Note that these conditions are sufficient conditions; i.e., we cannot judge whether the frame has a finite mechanism or not when none of (30a) or (30b) is satisfied; e.g., for $(\nu, \mu) = (A_1, A_1)$. Regarding the pairs (ν, μ) that do not satisfy either of (30a) or (30b), they give no judgment about the finiteness of mechanism. However, it is worth noting that in some specific cases we can judge whether $\hat{C}(\xi)$ is an even or odd function. For example, for the pair $(\nu, \mu) = (A_2, A_1)$, $\hat{C}(\xi)$ is an even function because there exists an element $h \in \mathrm{D}_n$ satisfying $T^\nu(h) = -1$ and $S^\mu(h) = 1$ and the following relation is satisfied:

$$\hat{C}(\xi) = \hat{C}(-\xi). \tag{31}$$

Similarly, for the pair $(\nu, \mu) = (A_2, A_2)$, $\hat{C}(\xi)$ is an odd function because there exists an h satisfying $T^\nu(h) = -1$ and $S^\mu(h) = -1$ and the following equation holds:

$$-\hat{C}(\xi) = \hat{C}(-\xi). \tag{32}$$

3.3 Finite mechanism with multiple generalized self-equilibrium force modes

3.3.1 Multiple generalized self-equilibrium force modes

Next we consider the case $q \geq 2$; i.e., there exist multiple generalized self-equilibrium force modes $\boldsymbol{\zeta}_1, \dots, \boldsymbol{\zeta}_q$. Define $Z_0 \in \mathbb{R}^{m \times q}$ by $Z_0 = [\boldsymbol{\zeta}_1, \dots, \boldsymbol{\zeta}_q]$.

Then, pre-multiplying $Z_0^\top$ and post-multiplying Z_0 to each of $S(r)$ and $S(s)$, we define $\hat{S}(r)$ and $\hat{S}(s) \in \mathbb{R}^{q\times q}$ by

$$\hat{S}(r) = Z_0^\top S(r) Z_0, \tag{33a}$$
$$\hat{S}(s) = Z_0^\top S(s) Z_0. \tag{33b}$$

It is easy to confirm that $\hat{S}(r)$ and $\hat{S}(s)$ are orthogonal matrices. Therefore, $\hat{S}(r)$ and $\hat{S}(s)$ are transformed from block diagonal matrices $\hat{S}^M(g)$ $(g \in \mathrm{D}_n)$ with an orthogonal matrix $Q \in \mathbb{R}^{q\times q}$ as

$$\hat{S}(r) = Q\hat{S}^M(r)Q^{-1}, \tag{34a}$$
$$\hat{S}(s) = Q\hat{S}^M(s)Q^{-1}, \tag{34b}$$

where M denotes the set of irreducible indices included in $\hat{S}(g)$. Note that, since $\hat{S}(g)$ is a representation matrix of dihedral symmetry, block diagonal components of $\hat{S}^M(g)$ are irreducible representation matrices of D_n.

Pre-multiplying Z_0 to Q, we define another orthonormal basis $\overline{Z}_0 = [\overline{\boldsymbol{\zeta}}_1, \dots, \overline{\boldsymbol{\zeta}}_q]$ as

$$\overline{Z}_0 = Z_0 Q. \tag{35}$$

Then, in a manner similar to (17a), the following lemma holds.

Lemma 1. *$\hat{S}^\mu(r), \hat{S}^\mu(s)$ and $\bar{Z}_0$ satisfy the following equations:*

$$S(r)\overline{Z}_0 = \overline{Z}_0\hat{S}^M(r), \tag{36a}$$
$$S(s)\overline{Z}_0 = \overline{Z}_0\hat{S}^M(s). \tag{36b}$$

Proof. Pre-multiplying Z_0 and post-multiplying $Z_0^\top$ to (34a) and (34b), and using (33a), (33b) and (35), we can show that the following equations hold:

$$Z_0 Z_0^\top S(r) Z_0 Z_0^\top = \overline{Z}_0 \hat{S}^M(r) \overline{Z}_0^\top, \tag{37a}$$
$$Z_0 Z_0^\top S(s) Z_0 Z_0^\top = \overline{Z}_0 \hat{S}^M(s) \overline{Z}_0^\top. \tag{37b}$$

Post-multiplying $\overline{Z}_0$ to both sides of (37a), and using $P = Z_0 Z_0^\top$ and $Z_0^\top Z_0 = \overline{Z}_0^\top \overline{Z}_0 = I$, we can rewrite the left-hand side and right-hand side of (37a) as

$$Z_0 Z_0^\top S(r) Z_0 Z_0^\top \overline{Z}_0 = PS(r) Z_0 Z_0^\top Z_0 Q = S(r)\overline{Z}_0, \tag{38a}$$
$$\bar{Z}_0 \hat{S}^M(r) \bar{Z}_0^\top \bar{Z}_0 = \bar{Z}_0 \hat{S}^M(r). \tag{38b}$$

This completes the proof of (36a). Eq. (36b) can be shown in the same manner. □

From Lemma 1, the group equivariance expressed by the reduced representation matrix $\hat{S}(g)$ in (16) can also be expressed by $\hat{S}^{\mu}(g)$ with the use of $\overline{Z}_0 = [\overline{\boldsymbol{\zeta}}_1, \dots, \overline{\boldsymbol{\zeta}}_q]$ satisfying (36a) and (36b) instead of using $Z_0 = [\boldsymbol{\zeta}_1, \dots, \boldsymbol{\zeta}_q]$ which satisfies (17a).

Hereinafter, we derive a condition for existence of a finite mechanism when $q \geq 2$ under the assumption that Q and $\hat{S}^M(g)$ are obtained explicitly. First, we consider the case $q = 2$, where $\hat{S}^M(g)$ is a 2×2 matrix which is expressed by either two 1×1 irreducible matrices or one 2×2 irreducible matrix. These two cases are studied separately, followed by the case $q \geq 3$.

It is important to know the numbers of irreducible representation indices included in $\hat{S}^M(g)$. Although it is difficult to calculate the numbers in general, we show how to obtain them in Sec. 3.3.5.

3.3.2 Case $q = 2$

Two one-dimensional irreducible representations

When $\hat{S}^M(g)$ includes two one-dimensional irreducible representations, two indices of them are expressed as $\mu_1, \mu_2 \in \{A_1, A_2, B_1, B_2\}$, and $\hat{S}^M(g)$ is defined as

$$\hat{S}^M(g) = \begin{bmatrix} S^{\mu_1}(g) & 0 \\ 0 & S^{\mu_2}(g) \end{bmatrix}. \tag{39}$$

In this case, using $\overline{\boldsymbol{\zeta}}_1$ and $\overline{\boldsymbol{\zeta}}_2$ instead of $\boldsymbol{\zeta}_1$ and $\boldsymbol{\zeta}_2$ in (14), we see that (21) is expressed as

$$\begin{bmatrix} S^{\mu_1}(g) & 0 \\ 0 & S^{\mu_2}(g) \end{bmatrix} \hat{\boldsymbol{C}}(\xi) = \hat{\boldsymbol{C}}(T^{\nu}(g)\xi), \ \ g \in \mathrm{D}_n, \tag{40}$$

equivalently,

$$S^{\mu_1}(g)\hat{C}_1(\xi) = \hat{C}_1(T^{\nu}(g)\xi), \ \ g \in \mathrm{D}_n, \tag{41a}$$

$$S^{\mu_2}(g)\hat{C}_2(\xi) = \hat{C}_2(T^{\nu}(g)\xi), \ \ g \in \mathrm{D}_n. \tag{41b}$$

Therefore, in a manner similar to the case $q = 1$, it is shown that if two combinations (ν, μ_1) and (ν, μ_2) are both included in (30a) and (30b), the frame has a finite mechanism because $\hat{\boldsymbol{C}}(\xi) = [\hat{C}_1(\xi), \hat{C}_2(\xi)]^{\top} = \boldsymbol{0}$ is obtained from (41a) and (41b).

Note that if there exists an $h \in \mathrm{D}_n$ satisfying $(T^{\nu}(h), S^{\mu_1}(h)) = (T^{\nu}(h), S^{\mu_2}(h)) = (-1, 1)$, then $\hat{\boldsymbol{C}}(\xi)$ is an even function. Similarly, if there exists an $h \in \mathrm{D}_n$ satisfying $(T^{\nu}(h), S^{\mu_1}(h)) = (T^{\nu}(h), S^{\mu_2}(h)) = (-1, -1)$, then $\hat{\boldsymbol{C}}(\xi)$ is an odd function. As mentioned in Sec. 3.2, we summarized these conditions here because they are useful for understanding symmetry property of the mechanism, although they give us no information about whether the frame has a finite mechanism mode or not.

One two-dimensional irreducible representation

If $\hat{S}^M(g)$ includes one two-dimensional irreducible representation, its indices are denoted as E_j $(j = 1, \dots, l)$ where l is defined as

$$l = (n-2)/2 \quad (\text{for } n \text{ even}), \tag{42a}$$

$$l = (n-1)/2 \quad (\text{for } n \text{ odd}), \tag{42b}$$

and the following equation holds:

$$\hat{S}^\mu(g) = S^{E_j}(g). \tag{43}$$

Here, the two-dimensional irreducible representation matrices are expressed as

$$S^{E_j}(r) = \begin{bmatrix} \cos(2\pi j/n) & -\sin(2\pi j/n) \\ \sin(2\pi j/n) & \cos(2\pi j/n) \end{bmatrix}, \quad S^{E_j}(s) = \begin{bmatrix} 1 & 0 \\ 0 & -1 \end{bmatrix}. \tag{44}$$

Hereinafter, we write $c_{j/n} = \cos(2\pi j/n), s_{j/n} = \sin(2\pi j/n)$.

Observe that (21) is expressed as

$$S^{E_j}(g)\hat{\boldsymbol{C}}(\xi) = \hat{\boldsymbol{C}}(T^\nu(g)\xi), \;\; g \in \mathrm{D}_n, \tag{45}$$

where $\nu \in \{A_1, A_2, B_1, B_2\}$. We study these four cases separately in the following part.

(1) $\nu = A_1$ *or* $\nu = A_2$

In this case, the infinitesimal mechanism mode has rotational symmetry through action r, and hence $T^{A_1}(r) = T^{A_2}(r) = 1$ holds. Thus, substituting $g = r$ to (45), we obtain

$$\begin{bmatrix} c_{j/n} - 1 & -s_{j/n} \\ s_{j/n} & c_{j/n} - 1 \end{bmatrix} \begin{bmatrix} \hat{C}_1(\xi) \\ \hat{C}_2(\xi) \end{bmatrix} = \begin{bmatrix} 0 \\ 0 \end{bmatrix}. \tag{46}$$

Since the determinant of the coefficient matrix in the left-hand side of (46) is $2(1 - c_{j/n}) > 0$, we obtain $\hat{C}_1(\xi) = \hat{C}_2(\xi) = 0$. Hence, the frame has a finite mechanism mode.

(2) $\nu = B_1$

In this case, $T^{B_1}(r) = -1$ and $T^{B_1}(s) = 1$ hold. Substituting $g = r$ and s, we can express (45) as follows:

$$\begin{bmatrix} c_{j/n} & -s_{j/n} \\ s_{j/n} & c_{j/n} \end{bmatrix} \begin{bmatrix} \hat{C}_1(\xi) \\ \hat{C}_2(\xi) \end{bmatrix} = \begin{bmatrix} \hat{C}_1(-\xi) \\ \hat{C}_2(-\xi) \end{bmatrix}, \tag{47a}$$

$$\begin{bmatrix} 1 & 0 \\ 0 & -1 \end{bmatrix} \begin{bmatrix} \hat{C}_1(\xi) \\ \hat{C}_2(\xi) \end{bmatrix} = \begin{bmatrix} \hat{C}_1(\xi) \\ \hat{C}_2(\xi) \end{bmatrix}. \tag{47b}$$

The second equation of (47b) shows that $\hat{C}_2(\xi) = 0$ is satisfied for any ξ. Substituting $\hat{C}_2(\xi) = \hat{C}_2(-\xi) = 0$ into (47a), we obtain $\hat{C}_1(\xi) = 0$. Accordingly, the frame has a finite mechanism mode.

(3) $\nu = B_2$

In this case, $T^{B_2}(r) = T^{B_2}(s) = -1$, and the following equations are obtained from (45) with $g = r$ and s:

$$\begin{bmatrix} c_{j/n} & -s_{j/n} \\ s_{j/n} & c_{j/n} \end{bmatrix} \begin{bmatrix} \hat{C}_1(\xi) \\ \hat{C}_2(\xi) \end{bmatrix} = \begin{bmatrix} \hat{C}_1(-\xi) \\ \hat{C}_2(-\xi) \end{bmatrix}, \tag{48a}$$

$$\begin{bmatrix} 1 & 0 \\ 0 & -1 \end{bmatrix} \begin{bmatrix} \hat{C}_1(\xi) \\ \hat{C}_2(\xi) \end{bmatrix} = \begin{bmatrix} \hat{C}_1(-\xi) \\ \hat{C}_2(-\xi) \end{bmatrix}. \tag{48b}$$

Eliminating $\hat{C}_1(-\xi)$ and $\hat{C}_2(-\xi)$ from (48a) and (48b), we obtain

$$\begin{bmatrix} c_{j/n} - 1 & -s_{j/n} \\ s_{j/n} & c_{j/n} + 1 \end{bmatrix} \begin{bmatrix} \hat{C}_1(\xi) \\ \hat{C}_2(\xi) \end{bmatrix} = \begin{bmatrix} 0 \\ 0 \end{bmatrix}. \tag{49}$$

Since the determinant of the coefficient matrix in the left-hand side of (49) is $(c_{j/n} - 1)(c_{j/n} + 1) + s_{j/n}^2 = 0$, (49) may have any non-zero solution satisfying

$$\hat{C}_2(\xi) = \frac{c_{j/n} - 1}{s_{j/n}} \hat{C}_1(\xi). \tag{50}$$

It is seen from (48b) that $\hat{C}_1(\xi)$ and $\hat{C}_2(\xi)$ are an even function and an odd function, respectively. Therefore, (50) implies $\hat{C}_1(\xi) = \hat{C}_2(\xi) = 0$, and hence the frame has a finite mechanism mode.

From the above results, when $\hat{S}^M(g)$ includes one two-dimensional irreducible representation, combinations of ν and μ for guaranteeing existence of a finite mechanism are summarized as follows:

$$\begin{aligned} (\nu, \mu) \in & \{(A_i, E_j) \mid i = 1, 2,\ j = 1, \ldots, l\} \\ & \cup \{(B_i, E_j) \mid i = 1, 2,\ j = 1, \ldots, l\}, \quad \text{(for } n \text{ even.)}, \end{aligned} \tag{51a}$$

$$(\nu, \mu) \in \{(A_i, E_j) \mid i = 1, 2,\ j = 1, \ldots, l\}, \quad \text{(for } n \text{ odd.)}. \tag{51b}$$

3.3.3 Summary of combinations (ν, μ) for existence of a finite mechanism for $q = 2$

Summarizing the results when $\hat{S}^M(g)$ includes two one-dimensional irreducible representations or one two-dimensional irreducible representation, combinations of ν and μ so that the frame has a finite mechanism is summarized in Table 1 with letter '$\circ$'. In Table 1, 'even' and 'odd' indicate that the corresponding $\hat{C}(\xi)$ are an even function and an odd function, respectively. These conditions are summarized here because they are useful for understanding the symmetry properties of the mechanism. It is noted that, if $\nu = \mu = A_1$, we cannot determine whether the frame has a finite mechanism or not, and whether the corresponding $\hat{C}(\xi)$ is an even function or an odd function.

Table 1 Combinations of ν and μ for existence of a finite mechanism

		μ				
		A_1	A_2	B_1	B_2	E_j
ν	A_1	unknown	$\circ$	$\circ$	$\circ$	$\circ$
	A_2	even	odd	$\circ$	$\circ$	$\circ$
	B_1	even	$\circ$	odd	$\circ$	$\circ$
	B_2	even	$\circ$	$\circ$	odd	$\circ$

3.3.4 Case $q \geq 3$

Next we consider the case $q \geq 3$. In this case, with block-diagonalized representation matrix $\hat{S}^M(g)$, (21) can be expressed as follows:

$$\begin{bmatrix} \ddots & & \\ & \hat{S}^{\mu_k}(g) & \\ & & \ddots \end{bmatrix} \begin{bmatrix} \vdots \\ \hat{C}_t(\xi) \\ \vdots \end{bmatrix} = \begin{bmatrix} \vdots \\ \hat{C}_t(T^\nu(g)(\xi)) \\ \vdots \end{bmatrix}, \quad (\text{for } \mu_k \in \{A_1, A_2, B_1, B_2\}), \tag{52a}$$

$$\begin{bmatrix} \ddots & & \\ & \hat{S}^{\mu_k}(g) & \\ & & \ddots \end{bmatrix} \begin{bmatrix} \vdots \\ \hat{C}_t(\xi) \\ \hat{C}_{t+1}(\xi) \\ \vdots \end{bmatrix} = \begin{bmatrix} \vdots \\ \hat{C}_t(T^\nu(g)(\xi)) \\ \hat{C}_{t+1}(T^\nu(g)(\xi)) \\ \vdots \end{bmatrix}, \quad (\text{for } \mu_k \in \{E_1, \ldots, E_l\}). \tag{52b}$$

Here, $\mu_k \in M$ is the kth irreducible representation index in the set M of irreducible indices included in $\hat{S}(g)$.

From (52a) and (52b), we can see that if the kth combination (μ_k, ν) corresponds to any one of the cases indicated by '$\circ$' in Table 1, then $\hat{C}_t(\xi) = 0$ holds for $\mu_k \in \{A_1, A_2, B_1, B_2\}$, and $\hat{C}_t(\xi) = \hat{C}_{t+1}(\xi) = 0$ holds for $\mu_k \in \{E_1, \ldots, E_l\}$. Similarly, if all combinations $(\mu_1, \nu), (\mu_2, \nu), \ldots$ are indicated by '$\circ$' in Table 1, the frame has a finite mechanism. Thus, a sufficient condition for a finite mechanism has been derived.

3.3.5 Evaluation of irreducible representation indices included in generalized self-equilibrium force modes

In the previous section, we showed that sufficient conditions for existence of a finite mechanism for $q \geq 2$ can be derived, if all of the irreducible representation indices included in q generalized self-equilibrium force modes $\boldsymbol{\zeta}_1, \ldots, \boldsymbol{\zeta}_q$ are known. In this section, we present a method to evaluate the number of irreducible representation indices based on the multiplicity of irreducible representations included in generalized self-equilibrium force modes.

The multiplicity of irreducible representations is calculated from the multiplicity of eigenvalues of $\hat{S}(r)$ and $\hat{S}(s)$. Let $R(\mathrm{D}_n) = \{A_1, A_2, B_1, B_2, E_1, \ldots, E_l\}$

denote the set of irreducible representations of dihedral group D_n. Multiplicity of an irreducible index μ ($\in R(\mathrm{D}_n)$) in M is denoted by a^μ; $a^\mu = 0$ if $\mu \notin M$. Since $\hat{S}(r)$ and $\hat{S}(s)$ are orthogonal matrices, absolute values of eigenvalues of $\hat{S}(r)$ and $\hat{S}(s)$, which generally include complex numbers, are all 1.

As shown in (34a) and (34b), a basis $Z_0 = [\boldsymbol{\zeta}_1, \ldots, \boldsymbol{\zeta}_q]^\top$ can be converted to another basis $\overline{Z}_0 = [\overline{\boldsymbol{\zeta}}_1, \ldots, \overline{\boldsymbol{\zeta}}_q]^\top$ by an appropriate orthogonal matrix $Q \in \mathbb{R}^{q\times q}$ as [19]

$$\overline{Z}_0 = Z_0 Q, \tag{53}$$

which block-diagonalizes $\hat{S}(r)$ as

$$\hat{S}(r) = Q\hat{S}^M(r)Q^{-1}, \tag{54}$$

$$\hat{S}^M(r) = \left[\begin{array}{c|c|c|c|c|c|c} \hat{S}^{A_1}(r) & & & & & & \\ \hline & \hat{S}^{A_2}(r) & & & & & \\ \hline & & \hat{S}^{B_1}(r) & & & & \\ \hline & & & \hat{S}^{B_2}(r) & & & \\ \hline & & & & \hat{S}^{E_1}(r) & & \\ \hline & & & & & \ddots & \\ \hline & & & & & & \hat{S}^{E_l}(r) \end{array}\right] \in \mathbb{R}^{q\times q}. \tag{55}$$

In (55), $\hat{S}^\mu(r) \in \mathbb{R}^{a^\mu \times a^\mu}$ ($\mu = A_1, A_2, B_1, B_2$) denotes a diagonal matrix consisting of $S^\mu(r)$ in (26a)–(26d), i.e.,

$$\hat{S}^\mu(r) = \begin{bmatrix} S^\mu(r) & & \\ & \ddots & \\ & & S^\mu(r) \end{bmatrix} \in \mathbb{R}^{a^\mu \times a^\mu}, \quad (\mu = A_1, A_2, B_1, B_2), \tag{56}$$

$$S^{A_1}(r) = 1, \;\; S^{A_2}(r) = 1, \;\; S^{B_1}(r) = -1, \;\; S^{B_2}(r) = -1. \tag{57}$$

Similarly, in (55), $\hat{S}^{E_j}(r) \in \mathbb{R}^{2a^{E_j} \times 2a^{E_j}}$ ($j = 1, \ldots, l$) denotes a block-diagonal matrix consisting of $S^{E_j}(r)$ in (44), i.e.,

$$\hat{S}^{E_j}(r) = \begin{bmatrix} S^{E_j}(r) & & \\ & \ddots & \\ & & S^{E_j}(r) \end{bmatrix} \in \mathbb{R}^{2a^{E_j} \times 2a^{E_j}}, \quad (j = 1, \ldots, l), \tag{58}$$

$$S^{E_j}(r) = \begin{bmatrix} \cos(2\pi j/n) & -\sin(2\pi j/n) \\ \sin(2\pi j/n) & \cos(2\pi j/n) \end{bmatrix}, \quad (j = 1, \ldots, l). \tag{59}$$

In a manner similar to $\hat{S}(r)$, $\hat{S}(s)$ can also be block-diagonalized to $\hat{S}^M(s)$ by Q as

$$\hat{S}(s) = Q\hat{S}^M(s)Q^{-1}, \tag{60}$$

$$\hat{S}^M(s) = \begin{bmatrix} \hat{S}^{A_1}(s) & & & & & & \\ & \hat{S}^{A_2}(s) & & & & & \\ & & \hat{S}^{B_1}(s) & & & & \\ & & & \hat{S}^{B_2}(s) & & & \\ & & & & \hat{S}^{E_1}(s) & & \\ & & & & & \ddots & \\ & & & & & & \hat{S}^{E_l}(s) \end{bmatrix} \in \mathbb{R}^{q\times q}. \quad (61)$$

In (61), $\hat{S}^\mu(s) \in \mathbb{R}^{a^\mu \times a^\mu}$ $(\mu = A_1, A_2, B_1, B_2)$ denotes a diagonal matrix consisting of $S^\mu(s)$ in (26a)–(26d) as

$$\hat{S}^\mu(s) = \begin{bmatrix} S^\mu(s) & & \\ & \ddots & \\ & & S^\mu(s) \end{bmatrix} \in \mathbb{R}^{a^\mu \times a^\mu}, \quad (\mu = A_1, A_2, B_1, B_2), \quad (62)$$

$$S^{A_1}(s) = 1,\ S^{A_2}(s) = -1,\ S^{B_1}(s) = 1,\ S^{B_2}(s) = -1, \quad (63)$$

and $\hat{S}^{E_j}(s) \in \mathbb{R}^{2a^{E_j} \times 2a^{E_j}}$ $(j = 1, \ldots, l)$ in (61) represents a block-diagonal matrix consisting of $S^{E_j}(s)$ in (44) as

$$\hat{S}^{E_j}(s) = \begin{bmatrix} S^{E_j}(s) & & \\ & \ddots & \\ & & S^{E_j}(s) \end{bmatrix} \in \mathbb{R}^{2a^{E_j} \times 2a^{E_j}}, \quad (j = 1, \ldots, l), \quad (64)$$

$$S^{E_j}(s) = \begin{bmatrix} 1 & 0 \\ 0 & -1 \end{bmatrix}. \quad (65)$$

It should be noticed that the multiplicity a^μ of irreducible representation index $\mu \in R(\mathrm{D}_n)$ has the same value in (56), (58), (62) and (64). Because $\hat{S}(r)$ is an orthogonal matrix, eigenvalues of $\hat{S}(r)$ are any of 1, -1, ω_j and $\overline{\omega}_j$ $(j = 1, \ldots, l)$ allowing duplication, where ω_j is a complex number defined with $i = \sqrt{-1}$ as

$$\omega_j = \cos(2\pi j/n) + i \sin(2\pi j/n), \quad (66)$$

and $\overline{\omega}_j$ denotes the conjugate complex number of ω_j. By contrast, the eigenvalues of an orthogonal matrix $\hat{S}(s)$ are either of 1 and -1.

We may compute the eigenvalues of $\hat{S}(r)$ and $\hat{S}(s)$ instead of $\hat{S}^M(r)$ and $\hat{S}^M(s)$ because eigenvalues do not change with respect to a similarity transformation with matrix Q. Let $N_r(1)$, $N_r(-1)$ and $N_r(\omega_j)$ denote the multiplicities of eigenvalues 1, -1 and ω_j $(j = 1, \ldots, l)$ of $\hat{S}(r)$, respectively. Similarly, we use $N_s(1)$ and $N_s(-1)$ to denote the multiplicities of eigenvalues 1 and -1 of $\hat{S}(s)$, respectively. Then, the following relations hold for the multiplicities a^μ

of irreducible representation indices:

$$a^{A_1} + a^{A_2} = N_r(1), \tag{67a}$$
$$a^{B_1} + a^{B_2} = N_r(-1), \tag{67b}$$
$$a^{E_j} = N_r(\omega_j), \quad (j = 1, \dots, l), \tag{67c}$$
$$a^{A_1} + a^{B_1} + \sum_{j=1}^{l} a^{E_j}(\omega_j) = N_s(1), \tag{67d}$$
$$a^{A_2} + a^{B_2} + \sum_{j=1}^{l} a^{E_j}(\omega_j) = N_s(-1). \tag{67e}$$

Besides, the following equations hold:

$$N_r(1) + N_r(-1) + 2\sum_{j=1}^{l} N_r(\omega_j) = q, \tag{68a}$$
$$N_s(1) + N_s(-1) = q. \tag{68b}$$

From (67c), a^{E_j} can be determined. Then, simplifying the other four equations (67a), (67b), (67d) and (67e), we obtain the following system of equations:

$$\begin{bmatrix} 1 & 1 & 0 & 0 \\ 0 & 0 & 1 & 1 \\ 1 & 0 & 1 & 0 \\ 0 & 1 & 0 & 1 \end{bmatrix} \begin{bmatrix} a^{A_1} \\ a^{A_2} \\ a^{B_1} \\ a^{B_2} \end{bmatrix} = \begin{bmatrix} N_r(1) \\ N_r(-1) \\ N_s(1) - \sum_{j=1}^{l} N_r(\omega_j) \\ N_s(-1) - \sum_{j=1}^{l} N_r(\omega_j) \end{bmatrix}. \tag{69}$$

Rank of the coefficient matrix in the left-hand side of (69) is 3; therefore, we cannot solve (69) for $a^{A_1}, a^{A_2}, a^{B_1}, a^{B_2}$ in general, and we focus on the special case where $a^{A_1}, a^{A_2}, a^{B_1}, a^{B_2}$ can be determined from (69).

From (69), a^{A_2}, a^{B_1} and a^{B_2} can be expressed with a^{A_1} as follows:

$$a^{A_2} = -a^{A_1} + N_r(1), \tag{70a}$$
$$a^{B_1} = -a^{A_1} + N_s(1) - \sum_{j=1}^{l} N_r(\omega_j), \tag{70b}$$
$$a^{B_2} = a^{A_1} + N_s(-1) - N_r(1) - \sum_{j=1}^{l} N_r(\omega_j). \tag{70c}$$

Because a^{μ} is an integer greater than or equal to 0, we obtain the following inequalities from (70a)–(70c):

$$\max\left\{0, N_r(1) - N_s(-1) + \sum_{j=1}^{l} N_r(\omega_j)\right\} \le a^{A_1} \le \min\left\{N_r(1), N_s(1) - \sum_{j=1}^{l} N_r(\omega_j)\right\}. \tag{71}$$

Therefore, if a^{A_1} is determined from (71), we can calculate other unknown variables $a^{A_2}, a^{B_1}, a^{B_2}$ from (70a)–(70c).

As we mentioned in Sec. 3.3.4, the sufficient condition guaranteeing that the frame has a finite mechanism is that '∘' should be specified for all combinations of $\mu \in M$ and ν in Table 1, where ν is the irreducible representation index of the infinitesimal mechanism mode. That is, in other words, for each ν, all $\mu \in R(\mathrm{D}_n)$ which do not correspond to '∘' in Table 1 must satisfy $a^\mu = 0$. The sufficient conditions are classified by ν as follows:

$$\nu = A_1 \implies a^{A_1} = 0, \tag{72a}$$

$$\nu = A_2 \implies a^{A_1} = a^{A_2} = 0, \tag{72b}$$

$$\nu = B_1 \implies a^{A_1} = a^{B_1} = 0, \tag{72c}$$

$$\nu = B_2 \implies a^{A_1} = a^{B_2} = 0. \tag{72d}$$

4 Numerical Examples

4.1 Example 1: 12-bar linkage ($G = \mathrm{D}_4$, $p = 1, q = 1$)

Existence of a finite mechanism is investigated for a square grid model in xy-plane as shown in Fig. 3. This model has D_4 symmetry, and the number of members m_0 is 12 and the number of nodes n_0 is 9. In Fig. 3, the numbers in ( ) and ⟨ ⟩ express indices of bars and nodes, respectively, and the notations [DX, DY, DZ, RX, RY, RZ] represent support conditions of translation and rotation; the first characters 'D' and 'R' indicate that displacement and rotation, respectively, are fixed, and the second characters 'X', 'Y' and 'Z' represent the direction or axis of rotation. Accordingly, the number of support conditions c of this frame is 10. The arrows t^1 and t^2 show local coordinate system of each of bar, and t^3 is perpendicular to the plane.

Hinge joints are added at some bar-ends of the frame expressed by dashed-lines in Fig. 3. Direction vectors of each of rotational hinges are also shown by [ ], where only the directions of hinges in the first quadrant are shown and others may be defined based on D_4 symmetry.

The first end of bar 1 at node 1 has a revolute joint around the axis $\boldsymbol{f}_{1,1} = [0,1,0]^\top$. On the other hand, the first end of bar 5 at node 2 has two revolute joints, i.e., a universal joint, which rotate around the axes $\boldsymbol{f}^1_{5,1} = [1,0,0]^\top$ and $\boldsymbol{f}^2_{5,1} = [0,0,1]^\top$ that are mutually orthogonal. In Fig. 3, the number of revolute joints and universal joints, denoted as h_1 and h_2, respectively, are 12 and 8. Consequently, the number of axes of hinges h is calculated as $h = h_1 + 2h_2 = 28$.

The number of components of compatibility vector is $m = 12m_0 - h = 144 - 28 = 116$, and the number of degrees of freedom is $f = 6n_0 + 6m_0 - c = 116$. From the Singular Value Decomposition (SVD) of $\mathit{\Gamma}_*$, we obtain $u = \mathrm{rank}(\mathit{\Gamma}_*) = 115$, and consequently, $p = f - u = 1$ and $q = m - u = 1$ are

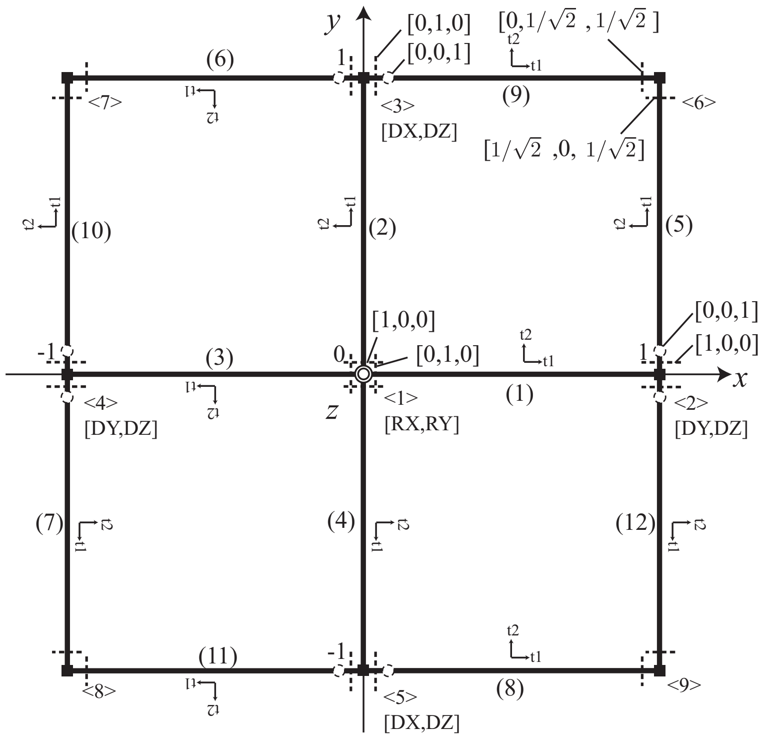

Fig. 3 12-bar linkage

determined. That is, the frame has one infinitesimal mechanism mode $\boldsymbol{\eta}_1$ and one generalized self-equilibrium force mode $\boldsymbol{\zeta}_1$, which are shown in Fig. 4.

Symmetry of $\boldsymbol{\eta}_1$

First, we derive matrix representations $T(r)$ and $T(s)$ to investigate the symmetry of infinitesimal mechanism mode $\boldsymbol{\eta}_1$. All nodes and center points of bars are classified using the *orbit* [2]. For example, if point k moves to point l by an action $h \in \mathrm{D}_n$, then points k and l are in the same orbit. All nodes and center points belong to any one of orbits, respectively, and small representation matrices are easily obtained for each orbit, which are assembled into a single representation matrix for the whole nodes and center points of bars. Furthermore, for D_n symmetry, all orbits are classified into at most four types 0, $1M$, $1V$ and 2 as described below, and the orbits with the same type have the same representation matrix.

For the 12-bar linkage in Fig. 3, nine nodes and 12 center points of bars are decomposed into four orbits as shown in Figs. 5–8.

Point on orbit 0 Orbit 0 consists of node 1, which is the only one node on z-axis as shown in Fig. 5. The components of displacement vector of the orbit is

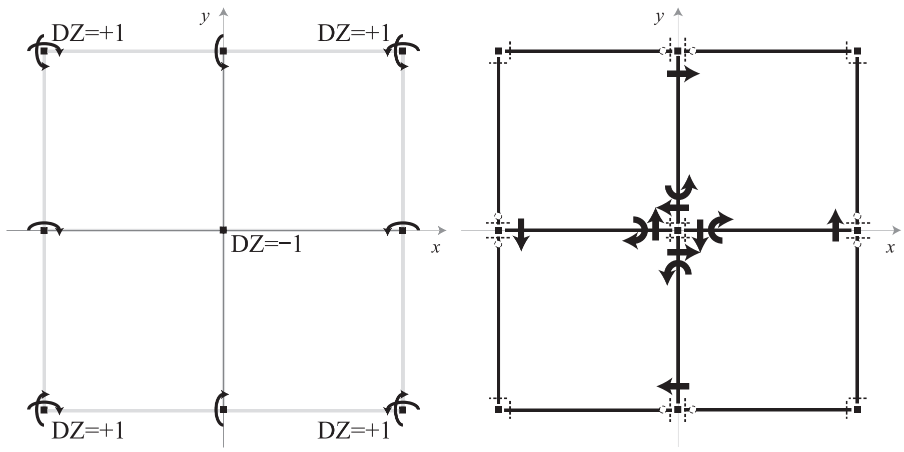

(a) (b)

Fig. 4 Infinitesimal mechanism mode and generalized self-equilibrium force mode of the 12-bar linkage; (a) Infinitesimal displacement mode $\boldsymbol{\eta}_1$, (b) Generalized self-equilibrium force mode $\boldsymbol{\zeta}_1$

decomposed into four types, $(0, xy, T), (0, z, T), (0, xy, R)$ and $(0, z, R)$, which correspond to translation in xy plane $[U_1^1, U_1^2]^\top$, translation in z-direction U_1^3, rotation around x- or y-axis $[\Theta_1^1, \Theta_1^2]^\top$, and rotation around z-axis Θ_1^3.

Matrix representations of action r and s of these four types are denoted as $T_{(0,xy,T)}(g) \in \mathbb{R}^{2\times 2}$, $T_{(0,z,T)}(g) \in \mathbb{R}^{1\times 1}$, $T_{(0,xy,R)}(g) \in \mathbb{R}^{2\times 2}$ and $T_{(0,z,R)}(g) \in \mathbb{R}^{1\times 1}$ as follows:

$$T_{(\kappa_1,\kappa_2,\kappa_3)}(g) = T_{\kappa_1}(g) \otimes T_{\kappa_2}(g) \otimes T_{\kappa_3}(g), \quad g \in G, \tag{73}$$

where $\otimes$ represents the Kronecker product, and κ_1, κ_2 and κ_3 are defined as

$$\kappa_1 \in \{0, 1M, 1V, 2\}\,, \tag{74a}$$
$$\kappa_2 \in \{xy, z\}\,, \tag{74b}$$
$$\kappa_3 \in \{T, R\}\,. \tag{74c}$$

The matrices in (73) are given as follows, where '0' in matrices are not written below:

$$T_0(r) = 1, \quad T_0(s) = 1, \tag{75}$$

$$T_{xy}(r) = \begin{bmatrix} \cos(\pi/2) & -\sin(\pi/2) \\ \sin(\pi/2) & \cos(\pi/2) \end{bmatrix}, \quad T_{xy}(s) = \begin{bmatrix} 1 & \\ & -1 \end{bmatrix}, \tag{76}$$

$$T_z(r) = 1, \quad T_z(s) = 1, \tag{77}$$

$$T_T(r) = 1, \quad T_T(s) = 1, \tag{78}$$

$$T_R(r) = 1, \quad T_R(s) = -1. \tag{79}$$

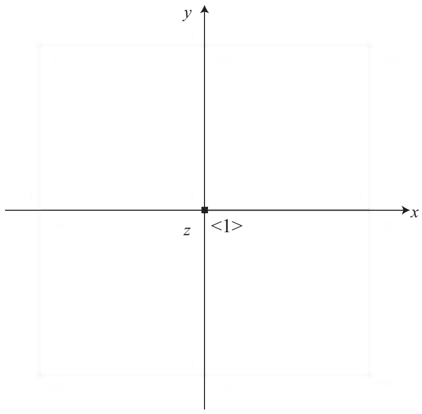

Fig. 5 Points on orbit 0

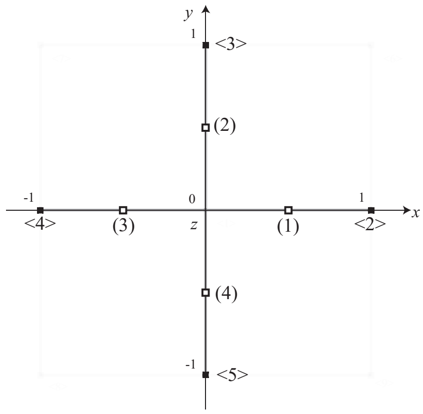

Fig. 6 Points on orbit $1V$

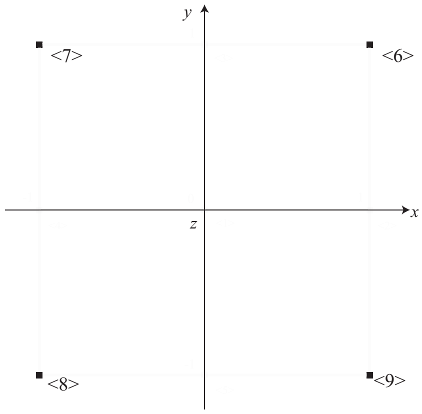

Fig. 7 Points on orbit $1M$

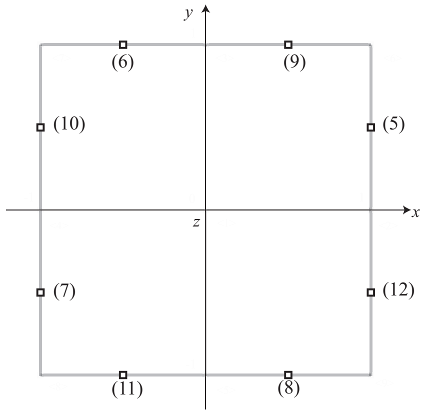

Fig. 8 Points on orbit 2

Points on orbit $1V$ Orbit $1V$ consists of nodes 2 through 5. Center points of bars 1 through 4 are also on another orbit $1V$ as shown in Fig. 6.

Displacements of nodes on orbit $1V$ are classified into four types in the same manner as orbit 0. Matrix representations corresponding to these four types, $T_{(1V,xy,T)}, T_{(1V,xy,R)}, T_{(1V,z,T)}$ and $T_{(1V,z,R)}$, are calculated by (73), (76)–(79) and $T_{1V}(r)$ and $T_{1V}(s)$ defined as

$$T_{1V}(r) = \begin{bmatrix} & & & 1 \\ 1 & & & \\ & 1 & & \\ & & 1 & \end{bmatrix}, \quad T_{1V}(s) = \begin{bmatrix} 1 & & & \\ & & & 1 \\ & & 1 & \\ & 1 & & \end{bmatrix}. \tag{80}$$

Points on orbit $1M$ Orbit $1M$ consists of four nodes 6 through 9 as shown in Fig. 7. The matrix representations of four types $T_{(1M,xy,T)}$, $T_{(1M,xy,R)}$, $T_{(1M,z,T)}$ and $T_{(1M,z,R)}$ are defined with $T_{1M}(r)$ and $T_{1M}(s)$, which are given as follows:

$$T_{1M}(r)=\begin{bmatrix} & & & 1\\ 1 & & & \\ & 1 & & \\ & & 1 & \end{bmatrix},\quad T_{1M}(s)=\begin{bmatrix} & & & 1\\ & & 1 & \\ & 1 & & \\ 1 & & & \end{bmatrix}. \tag{81}$$

Points on orbit 2 Finally, orbit 2 consists of eight center points of bars 5 through 12 as shown in Fig. 8. The matrix representations of four types $T_{(2,xy,T)}, T_{(2,xy,R)}, T_{(2,z,T)}$ and $T_{(2,z,R)}$ are calculated with $T_2(r)$ and $T_2(s)$ defined as

$$T_2(r)=\begin{bmatrix} & & & 1 & & & & \\ 1 & & & & & & & \\ & 1 & & & & & & \\ & & 1 & & & & & \\ & & & & & & & 1\\ & & & & 1 & & & \\ & & & & & 1 & & \\ & & & & & & 1 & \end{bmatrix},\quad T_2(s)=\begin{bmatrix} & & & & & & & 1\\ & & & & & & 1 & \\ & & & & & 1 & & \\ & & & & 1 & & & \\ & & & 1 & & & & \\ & & 1 & & & & & \\ & 1 & & & & & & \\ 1 & & & & & & & \end{bmatrix}. \tag{82}$$

All of $T_{(\kappa_1,\kappa_2,\kappa_3)}$ are assembled into $T(r)$ and $T(s)\in\mathbb{R}^{f\times f}$. With these matrices, we confirmed that $\boldsymbol{\eta}_1^\top T(r)\boldsymbol{\eta}_1=1$ and $\boldsymbol{\eta}_1^\top T(s)\boldsymbol{\eta}_1=1$, which means the infinitesimal mechanism mode vector $\boldsymbol{\eta}_1$ is symmetric with respect to both rotation r and reflection s. That is, the one-dimensional irreducible representation index of $\boldsymbol{\eta}_1$ is $\nu=A_1$.

Symmetry of $\boldsymbol{\zeta}_1$*:*

Next, we derive matrix representations $S(r)$ and $S(s)\in\mathbb{R}^{m\times m}$ to study the symmetry property of the generalized self-equilibrium force mode $\boldsymbol{\zeta}_1$. The 12 bars are decomposed into two orbits $1V$ and 2 as shown in Figs. 9–10.

For formulating the incompatibility vector $\boldsymbol{C}(\boldsymbol{W})$, we use Euler parameter for large rotation [13, 14]. Let $\Delta\boldsymbol{U}_{ij}=[\Delta U_{ij}^1,\Delta U_{ij}^2,\Delta U_{ij}^3]^\top$ and $\Delta\boldsymbol{\Theta}_{ij}=[\Delta\Theta_{ij}^1,\Delta\Theta_{ij}^2,\Delta\Theta_{ij}^3]^\top$ denote the components of translational and rotational incompatibility of the jth end of bar i in global coordinates, where the compatibility of revolute joint $\boldsymbol{e}_{ij}^{(2)}=\boldsymbol{0}$ or universal joint $e_{ij}^{(1)}=0$, is included instead of $\Delta\boldsymbol{\Theta}_{ij}$ at some bar-ends. See Appendix A.1 for detailed formulation of $\boldsymbol{C}(\boldsymbol{W})$.

Bars on orbit $1V$ Bars 1 through 4 are on an orbit $1V$ corresponding to eight translational compatibility on xy-plane $[\Delta U_{1j}^1,\Delta U_{1j}^2,\Delta U_{2j}^1,\Delta U_{2j}^2,\Delta U_{3j}^1,\Delta U_{3j}^2,\Delta U_{4j}^1,\Delta U_{4j}^2]^\top$ for each $j\in\{1,2\}$. This vector is rotated counterclockwise by the matrix representation $S_{(1V,xy,T)}(r)\in\mathbb{R}^{8\times 8}$ of the action r of type $(1V,xy,T)$, and reflected with respect to xy plane by the matrix representation $S_{(1V,xy,T)}(s)\in\mathbb{R}^{8\times 8}$ of the action s. We can define $S_{(1V,xy,T)}(r)$ and $S_{(1V,xy,T)}(s)$ as follows:

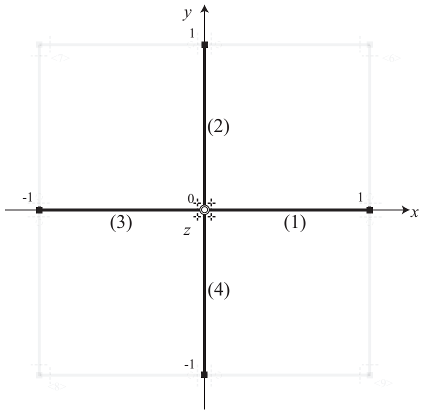

Fig. 9 Bars on orbit $1V$

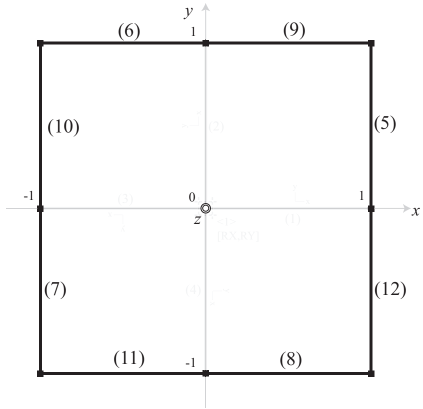

Fig. 10 Bars on orbit 2

$$S_{(\chi_1,\chi_2,\chi_3)}(g) = S_{\chi_1}(g) \otimes S_{\chi_2}(g) \otimes S_{\chi_3}(g), \quad g \in G, \tag{83}$$

$$S_{1V}(r) = \begin{bmatrix} & & & 1 \\ 1 & & & \\ & 1 & & \\ & & 1 & \end{bmatrix}, \quad S_{1V}(s) = \begin{bmatrix} 1 & & & \\ & & & 1 \\ & & 1 & \\ & 1 & & \end{bmatrix}, \tag{84}$$

$$S_{xy}(r) = \begin{bmatrix} \cos(\pi/2) & -\sin(\pi/2) \\ \sin(\pi/2) & \cos(\pi/2) \end{bmatrix}, \quad S_{xy}(s) = \begin{bmatrix} 1 & \\ & -1 \end{bmatrix}, \tag{85}$$

$$S_T(r) = 1, \quad S_T(s) = 1. \tag{86}$$

Similarly, four components of translational compatibility in z-direction $[\Delta U^3_{1j}, \Delta U^3_{2j}, \Delta U^3_{3j}, \Delta U^3_{4j}]^\top$ for each $j \in \{1,2\}$, which we call the components of type $(1V, z, T)$, are rotated by $S_{(1V,z,T)}(r) \in \mathbb{R}^{4\times 4}$ and reflected by $S_{(1V,z,T)}(s) \in \mathbb{R}^{4\times 4}$. These matrices are calculated by (83) with (84), (86), and $S_z(r)$ and $S_z(s)$ defined as

$$S_z(r) = 1, \quad S_z(s) = 1. \tag{87}$$

Eight components of type $(1V, xy, R)$ rotational compatibility around x- or y-axis at bar-ends are defined as $[\Delta\Theta^1_{1j}, \Delta\Theta^2_{1j}, \Delta\Theta^1_{2j}, \Delta\Theta^2_{2j}, \Delta\Theta^1_{3j}, \Delta\Theta^2_{3j}, \Delta\Theta^1_{4j}, \Delta\Theta^2_{4j}]^\top$ for each $j \in \{1,2\}$. We define $S_{(1V,xy,R)}(r) \in \mathbb{R}^{8\times 8}$ and $S_{(1V,xy,R)}(s) \in \mathbb{R}^{8\times 8}$ for the components of type $(1V, z, R)$ by (84), (87), and $S_R(r)$ and $S_R(s)$ as

$$S_R(r) = 1, \quad S_R(s) = -1. \tag{88}$$

Representation matrices corresponding to the compatibility of revolute joints are to be satisfied at the first ends of members 1 through 4. We convert

$\boldsymbol{e}_{ij} = \boldsymbol{f}^b_{ij} \times \boldsymbol{f}^n_{ij}$ to the values $\tilde{e}^1_{ij}, \tilde{e}^2_{ij}, \tilde{e}^3_{ij}$ in local coordinates of each member, as follows, to define symmetry using the same two components for all members:

$$\tilde{e}^1_{ij} = \boldsymbol{e}^\top_{ij}\boldsymbol{t}^1_i, \quad \tilde{e}^2_{ij} = \boldsymbol{e}^\top_{ij}\boldsymbol{t}^2_i, \quad \tilde{e}^3_{ij} = \boldsymbol{e}^\top_{ij}\boldsymbol{t}^3_i, \tag{89}$$

where $\boldsymbol{t}^2_i$ and $\boldsymbol{t}^3_i$ are defined to satisfy $\boldsymbol{t}^2_i = \boldsymbol{n}_z \times \boldsymbol{t}^1_i$ and $\boldsymbol{t}^3_i = \boldsymbol{t}^1_i \times \boldsymbol{t}^2_i$, in which $\boldsymbol{n}_z$ is a unit vector in the direction of z axis. Using (89), the pairs of components for assigning compatibility conditions in two axes are classified into $(\tilde{e}^1, \tilde{e}^2), (\tilde{e}^1, \tilde{e}^3)$ and $(\tilde{e}^2, \tilde{e}^3)$.

When the pair $(\tilde{e}^1, \tilde{e}^2)$ is selected, we name this type $(1V, \tilde{e}^1\tilde{e}^2, R)$. Then, corresponding representation matrices $S_{(1V,\tilde{e}^1\tilde{e}^2,R)}(r)$ and $S_{(1V,\tilde{e}^1\tilde{e}^2,R)}(s)$ can be calculated using $S_{\tilde{e}^1\tilde{e}^2}(r)$ and $S_{\tilde{e}^1\tilde{e}^2}(s)$ defined as

$$S_{\tilde{e}^1\tilde{e}^2}(r) = \begin{bmatrix} 1 & \\ & 1 \end{bmatrix}, \quad S_{\tilde{e}^1\tilde{e}^2}(s) = \begin{bmatrix} 1 & \\ & -1 \end{bmatrix}. \tag{90}$$

If $(\tilde{e}^1, \tilde{e}^3)$ is chosen, we classify it into $(1V, \tilde{e}^1\tilde{e}^2, R)$. Similarly, combination $(\tilde{e}^2, \tilde{e}^3)$ is classified into $(1V, \tilde{e}^2\tilde{e}^3, R)$. $S_{\tilde{e}^1\tilde{e}^3}(r), S_{\tilde{e}^1\tilde{e}^3}(s)$, $S_{\tilde{e}^2\tilde{e}^3}(r)$ and $S_{\tilde{e}^2\tilde{e}^3}(s)$ used in the corresponding representation matrices $S_{(1V,\tilde{e}^1\tilde{e}^3,R)}(r)$, $S_{(1V,\tilde{e}^1\tilde{e}^3,R)}(s)$, $S_{(1V,\tilde{e}^2\tilde{e}^3,R)}(r)$ and $S_{(1V,\tilde{e}^2\tilde{e}^3,R)}(s)$ are expressed as follows:

$$S_{\tilde{e}^1\tilde{e}^3}(r) = \begin{bmatrix} 1 & \\ & 1 \end{bmatrix}, \quad S_{\tilde{e}^1\tilde{e}^3}(s) = \begin{bmatrix} 1 & \\ & 1 \end{bmatrix}, \tag{91}$$

$$S_{\tilde{e}^2\tilde{e}^3}(r) = \begin{bmatrix} 1 & \\ & 1 \end{bmatrix}, \quad S_{\tilde{e}^2\tilde{e}^3}(s) = \begin{bmatrix} -1 & \\ & 1 \end{bmatrix}. \tag{92}$$

Bars on orbit 2 Next, we focus on another orbit called orbit 2 corresponding to bars $5, \dots, 12$ in Fig. 10. In the same manner as orbit 1, we decompose components of compatibilities on the orbit 2 into four types, $(2, xy, T)$, $(2, z, T)$, $(2, xy, R)$ and $(2, z, R)$. The corresponding matrix representations are expressed by (85)–(88) and additional matrices $S_2(r)$ and $S_2(s)$ defined as follows:

$$S_2(r) = \begin{bmatrix} &&&1&&&& \\ 1&&&&&&& \\ &1&&&&&& \\ &&1&&&&& \\ &&&&&&&1 \\ &&&&1&&& \\ &&&&&1&& \\ &&&&&&1& \end{bmatrix}, \quad S_2(s) = \begin{bmatrix} &&&&&&&1 \\ &&&&&&1& \\ &&&&&1&& \\ &&&&1&&& \\ &&&1&&&& \\ &&1&&&&& \\ &1&&&&&& \\ 1&&&&&&& \end{bmatrix}. \tag{93}$$

Universal joints exist at the first ends of bars $5, \dots, 12$. The type of rotational compatibility of them, defined by $e^{(1)}_{ij}$ in (A5) is denoted as $(2, e, R)$. Here, $S_e(r)$ and $S_e(s)$ are expressed as follows:

$$S_e(r) = 1, \quad S_e(s) = 1. \tag{94}$$

Judgment of existence of finite mechanism

We assemble all $S_{(\chi_1,\chi_2,\chi_3)}(r)$ and $S_{(\chi_1,\chi_2,\chi_3)}(s)$ to formulate $S(r)$ and $S(s) \in \mathbb{R}^{m\times m}$, respectively. Pre-multiplying $\boldsymbol{\zeta}_1^\top$ and post-multiplying $\boldsymbol{\zeta}_1$ to these matrices, $\boldsymbol{\zeta}_1^\top S(r)\boldsymbol{\zeta}_1 = -1$ and $\boldsymbol{\zeta}_1^\top S(s)\boldsymbol{\zeta}_1 = -1$ are satisfied, which means the generalized self-equilibrium force vector $\boldsymbol{\zeta}_1$ is anti-symmetric with respect to both rotation action r and reflection action s. That is, the one-dimensional irreducible representation index of $\boldsymbol{\zeta}_1$ is $\mu = B_2$.

Consequently, we found that $(\nu, \mu) = (A_1, B_2)$, which is included in (30a). Hence, from (22a), we conclude that the frame has one finite mechanism mode.

4.2 Example 2: 12-bar linkage ($G = \mathrm{D}_4$, $p = 1, q = 2$)

For the model in Fig. 3, we consider another constraint which fixes the rotation around z-axis at node 1. In this model, c increases to 11. From the SVD of $\varGamma_*$, we find $u = 114$, and accordingly, $p = 1$ and $q = 2$; i.e., this model has one infinitesimal mechanism mode $\boldsymbol{\eta}_1$ and two generalized self-equilibrium force modes $\boldsymbol{\zeta}_1, \boldsymbol{\zeta}_2$. In this model, the symmetry of $\boldsymbol{\eta}_1$ represented by ν remains A_1, because $\boldsymbol{\eta}_1^\top T(r)\boldsymbol{\eta}_1 = 1$ and $\boldsymbol{\eta}_1^\top T(s)\boldsymbol{\eta}_1 = 1$ are satisfied. To study the symmetry of $\boldsymbol{Z}_0 = [\boldsymbol{\zeta}_1, \boldsymbol{\zeta}_2]$, we calculated the eigenvalues of $\hat{S}(r) = \boldsymbol{Z}_0^\top S(r)\boldsymbol{Z}_0$ and $\hat{S}(s) = \boldsymbol{Z}_0^\top S(s)\boldsymbol{Z}_0$, and found that the eigenvalues of $\hat{S}(r)$ are 1 and -1 (neither is multiple), and the eigenvalues of $\hat{S}(s)$ are -1 with multiplicity 2; i.e.,

$$N_r(1) = N_r(-1) = 1,\ N_r(\omega_1) = 0,\ N_s(1) = 0,\ N_s(-1) = 2. \tag{95}$$

which leads to $a^{E_1} = a^{E_2} = 0$. Substituting (95) into (71), we obtain

$$0 \le a^{A_1} \le 0, \quad \Rightarrow \quad a^{A_1} = 0, \tag{96}$$

and, consequently, other multiplicities a^{A_2}, a^{B_1} and a^{B_2} are calculated from (70a)–(70c) as

$$a^{A_2} = 1,\ a^{B_1} = 0,\ a^{B_2} = 1. \tag{97}$$

Therefore, we finally find $M = \{A_2, B_2\}$ and obtain two combinations of ν and $\mu_k \in M$, that is, $(\nu, \mu_1) = (A_1, A_2)$ and $(\nu, \mu_2) = (A_1, B_2)$. They are both included in (30a), which means this model satisfies the sufficient condition to have one finite mechanism.

4.3 Example 3: 6-bar linkage ($G = \mathrm{D}_3, p = 1, q = 1$)

Next, we consider 6-bar linkage which consists of $n_0 = 6$ nodes 1 through 6 and $m_0 = 6$ members as shown in Figs. 11 and 12. Each bar has hinges at both ends, and any two hinges connected to the same node are parallel. Note that the hinges are assigned duplicately to clearly investigate the symmetry property. A pair of hinges at the same node are combined to a single hinge, when making a physical model. All lines of the axes of hinges at nodes 1, 3 and

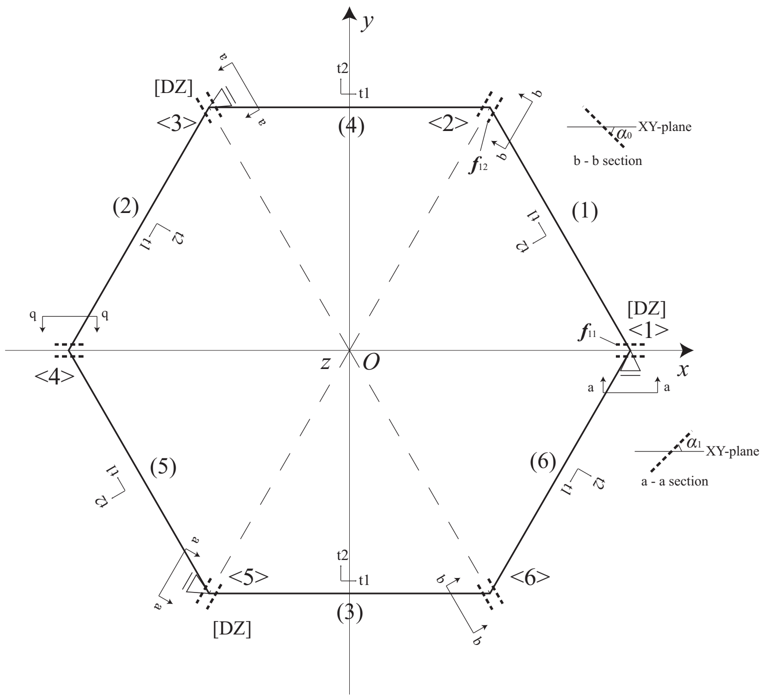

Fig. 11 6-bar linkage

5 intersect with z-axis at $(0, 0, -\tan\alpha_1)$, and all lines of the axes of hinges at nodes 2, 4 and 6 intersect with z-axis at $(0, 0, -\tan\alpha_0)$. Then, the direction vector $\boldsymbol{f}_{k_{ij}}$ of hinge axis between jth end of bar i and node k_{ij} is expressed as follows:

$$\boldsymbol{f}_{k_{ij}} = \begin{pmatrix} \cos\alpha_1 \cos\dfrac{(k_{ij}-1)\pi}{3} \\ \cos\alpha_1 \sin\dfrac{(k_{ij}-1)\pi}{3} \\ \sin\alpha_1 \end{pmatrix} \quad \text{for } k_{ij} = 1, 3, 5. \tag{98a}$$

$$\boldsymbol{f}_{k_{ij}} = \begin{pmatrix} \cos\alpha_0 \cos\dfrac{(k_{ij}-1)\pi}{3} \\ \cos\alpha_0 \sin\dfrac{(k_{ij}-1)\pi}{3} \\ \sin\alpha_0 \end{pmatrix} \quad \text{for } k_{ij} = 2, 4, 6. \tag{98b}$$

Let O denote the origin of coordinate axes. We use $\boldsymbol{l}_k^1, \boldsymbol{l}_k^2, \boldsymbol{l}_k^3$ to denote the unit vectors of local coordinate at node k, where $\boldsymbol{l}_k^1$ is the unit vector directed from O to node k and $\boldsymbol{l}_k^2$ and $\boldsymbol{l}_k^3$ satisfy $\boldsymbol{l}_k^2 = [0, 0, 1]^\top \times \boldsymbol{l}_k^1$ and $\boldsymbol{l}_k^3 = \boldsymbol{l}_k^1 \times \boldsymbol{l}_k^2$, respectively. Since rotation angles around the axes of two hinges connected to the same node is indefinite, we add the following compatibility equations with

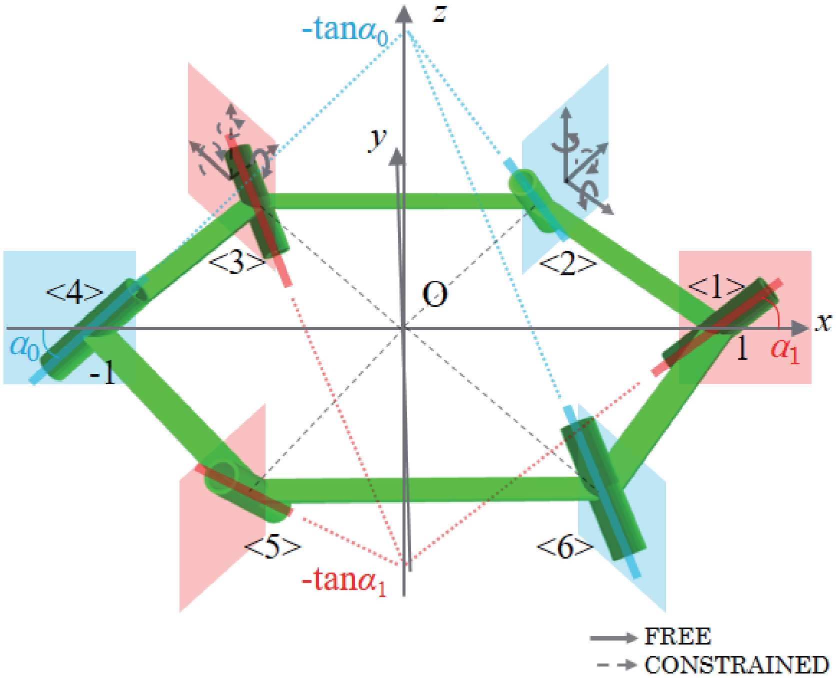

Fig. 12 Hinge directions of the 6-bar linkage

respect to $\boldsymbol{\Theta}_k$ $(k = 1, \ldots, 6)$ to prevent the indefiniteness:

$$\boldsymbol{l}_k^{1\top} \boldsymbol{\Theta}_k = 0, \ (k = 1, \ldots, 6). \tag{99}$$

In addition, at nodes 1, 3 and 5, translations $\boldsymbol{U}_k$ are allowed only along the diagonal directions passing through the origin O as

$$\boldsymbol{l}_k^{2\top} \boldsymbol{U}_k = 0, \ (k = 1, 3, 5), \tag{100a}$$

$$\boldsymbol{l}_k^{3\top} \boldsymbol{U}_k = 0, \ (k = 1, 3, 5). \tag{100b}$$

Assembling (99)–(100), the number of constraints c is 12. Then, m and f are calculated as $m = 12m_0 + c - h = 12 \times 6 + 12 - 12 = 72$ and $f = 6n_0 + 6m_0 = 6 \times 6 + 6 \times 6 = 72$, respectively. In this model, the support conditions are added to the compatibility conditions, because they are in diagonal directions, and it is difficult to eliminate them from the displacement components.

Considering conditions of the hinges and the support constraints, we can judge that the symmetry of this model is D_3. Note that nodes $1, 3$ and 5 are on orbit $1V$, nodes 2, 4 and 6 are on orbit $1M$, and all bars are on orbit 2. Then, representation matrices $T(g)$ and $S(g)$ of this model are obtained in a manner similar to the 12-bar linkage.

Let $\alpha_1 = \pi/4$ and $\alpha_0 = -\pi/4$. From the SVD of Γ_*, we obtain $u = \mathrm{rank}(\Gamma_*) = 71$. Accordingly, this linkage has one infinitesimal mechanism mode $\boldsymbol{\eta}_1$ and one generalized self-equilibrium force mode $\boldsymbol{\zeta}_1$, because $p = f - u = 1$ and $q = m - u = 1$. It has been confirmed that irreducible representation index of $\boldsymbol{\eta}_1$ is $\nu = A_1$, because $\boldsymbol{\eta}_1^\top T(r)\boldsymbol{\eta}_1 = 1$ and $\boldsymbol{\eta}_1^\top T(s)\boldsymbol{\eta}_1 = 1$. Moreover, irreducible representation index of $\boldsymbol{\zeta}_1$ is $\mu = A_2$, because $\boldsymbol{\zeta}_1^\top S(r)\boldsymbol{\zeta}_1 = 1$ and $\boldsymbol{\zeta}_1^\top S(s)\boldsymbol{\zeta}_1 = -1$. This combination of (ν, μ) is included in (30b), that is, this linkage has one finite mechanism mode.

Next, α_0 has been changed to $-\pi/2, -\pi/3, -\pi/6, 0, \pi/6, \pi/4$ and $\pi/3$, while keeping α_1 at $\pi/4$ For $\alpha_0 = -\pi/3, -\pi/6, \pi/6, \pi/3$, it has been confirmed in the same manner as $\alpha_0 = -\pi/4$ that this linkage has one finite mechanism. Therefore, this linkage is supposed to have one finite mechanism when $\alpha_1 \neq \alpha_0$. However, for $\alpha_0 = -\pi/2, 0$ and $\pi/4$, p becomes 4, 7 and 3, respectively, therefore we cannot apply the method proposed in this study.

4.4 Example 4: 6-bar linkage ($G = \mathrm{D}_3, p = 1, q = 4$)

Next, we consider another model by adding the following rotational constraints around z axis at nodes 1, 3 and 5 of the previous example:

$$\boldsymbol{l}_k^{3\top}\boldsymbol{\Theta}_k = 0, \ \ (k = 1, 3, 5). \tag{101}$$

These constraints change c and m to 15 and 75, respectively. Let $\alpha_1 = \pi/4$ and $\alpha_0 = -\pi/4$. By SVD, $u = 71$, and consequently, $p = 1$ and $q = 4$ are obtained. Therefore, this model has one infinitesimal mechanism mode and four generalized self-equilibrium force modes.

It is found that the irreducible representation index of $\boldsymbol{\eta}_1$ is still $\nu = A_1$. Then, to judge whether this model has one finite mechanism or not, we study M: the set of irreducible representation indices in four generalized self-equilibrium force modes $\boldsymbol{Z}_0 = [\boldsymbol{\zeta}_1, \ldots, \boldsymbol{\zeta}_4]$. From the eigenvalue analysis of $\hat{S}(r) = \boldsymbol{Z}_0^\top S(r)\boldsymbol{Z}_0$ and $\hat{S}(s) = \boldsymbol{Z}_0^\top S(s)\boldsymbol{Z}_0$, we obtain the multiplicity of the eigenvalues as follows:

$$N_r(1) = 2, \ N_r(-1) = 0, \ N_r(\omega_1) = 1, \ N_r(\overline{\omega}_1) = 1, \tag{102a}$$
$$N_s(1) = 1, \ N_s(-1) = 3, \tag{102b}$$

where $\omega_1 = \cos(2\pi/3) + i\sin(2\pi/3)$. Substituting (102a) and (102b) to (67a) and (67e), multiplicity of the irreducible representation indices in M are determined as

$$a^{A_1} = 0, \ a^{A_2} = 2, \ a^{B_1} = a^{B_2} = 0, \ a^{E_1} = 1. \tag{103}$$

Therefore, we find $M = \{A_2, A_2, E_1\}$, and that this model has three combinations of irreducible representation indices: $(\nu, \mu_1) = (\nu, \mu_2) = (A_1, A_2)$ and $(\nu, \mu_3) = (A_1, E_1)$. All of these combinations are included in (30b); therefore, this model has one finite mechanism.

5 Conclusion

In this paper, sufficient conditions for existence of finite mechanism have been derived for three-dimensional bar-hinge mechanisms with D_n symmetry.

The following properties hold for bar-hinge mechanisms with group G of geometrical transformations g:

1. Infinitesimal mechanism modes are defined as the basis vectors of null space of the linear compatibility matrix obtained by differentiating the compatibility equations and evaluating it at the undeformed state.
2. Generalized self-equilibrium force modes are defined as the basis vectors of kernel of the transpose of linear compatibility matrix.
3. The implicit function theorem ensures that the group equivariance property of the compatibility equations inherits to the reduced equations in the null space of the linear compatibility matrix.

Following properties hold for bar-hinge mechanisms with D_n symmetry and single infinitesimal mechanism mode:

1. The matrix representation of reduced compatibility equations turns out to be a scalar that is characterized by symmetry conditions of the mechanism mode.
2. If the bar-hinge mechanism has single generalized self-equilibrium force mode, the matrix representation of self-equilibrium force mode is also a scalar that is characterized by symmetry conditions of the self-equilibrium force mode.
3. Sufficient conditions for existence of finite mechanism are derived from the one-dimensional irreducible representations of mechanism mode and self-equilibrium force mode.
4. When there exist more than one self-equilibrium force mode, existence of finite mechanism depends on the symmetry properties of mechanism mode and self-equilibrium force modes. The combinations of one-dimensional matrix representation of mechanism mode and one- or two-dimensional matrix representation of self-equilibrium force mode are summarized in Table 1.

The results have been confirmed in the numerical examples of 12-bar square grid and a 6-bar ring mechanism.

References

1. A. Zingoni, Group-theoretic exploitations of symmetry in computational solid and structural mechanics, Int. J. Numer. Meth. Eng., Vol. 79, pp. 253–289, 2009.
2. K. Ikeda and K. Murota, Imperfect Bifurcation in Structures and Materials (2nd ed.), Applied Mathematical Sciences, Springer, 2010.
3. K. Ikeda, M. Ohsaki and Y. Kanno, Imperfection sensitivity of hilltop branching points of systems with dihedral group symmetry, Int. J. Non-Linear Mech., Vol. 40, pp. 755–774, 2005.
4. J. Y. Zhang, S. D. Guest and M. Ohsaki, Symmetric prismatic tensegrity structures: Part I. Configuration and stability, Int. J. Solids Struct., Vol. 45(1), pp. 1–14, 2009.

5. Y. Kanno, M. Ohsaki, K. Murota and N. Katoh, Group symmetry in interior-point methods for semidefinite program, Optim. Eng., Vol. 2, pp. 293–320, 2001.
6. Y. Chen and J. Feng, Generalized eigenvalue analysis of symmetric prestressed structures using group theory, J. Computing in Civil Eng., Vol. 26(4), pp. 488–497, 2012.
7. M. Ohsaki, Y. Kanno and S. Tsuda, Linear programming approach to design of spatial link mechanism with partially rigid joints, Struct. Multidisc. Optim., Vol. 50, pp. 945–956, 2014.
8. M. Ohsaki, S. Tsuda and Y. Miyazu, Design of linkage mechanisms of partially rigid frames using limit analysis with quadratic yields functions, Int. J. Solids and Struct., Vol. 88–89, pp. 68–78, 2016.
9. S. D. Guest and P. W. Fowler, Symmetry conditions and finite mechanisms, J. Mech. Mater. Struct., Vol. 2(2), pp. 293–301, 2007.
10. B. Schulze, S. D. Guest and P. W. Fowler, When a symmetric body-hinge structure isostatic?, Int. J. Solids Struct., Vol. 51, pp. 2157–2166, 2014.
11. R. Watada and M. Ohsaki, Series expansion method for determination of order of 3-dimensional bar-joint mechanism with arbitrarily inclined hinges, Int. J. Solids Struct., published online, doi: 10.1016/j.ijsolstr.2018.02.012, 2018.
12. R. Ikeshita, Bifurcation Analysis of Symmetric Mechanisms by using Group Theory (in Japanese), Graduation thesis, Department of Mathematical Engineering and Information Physics, School of Engineering, The University of Tokyo, February 2013.
13. H. Cheng and K. C. Gupta, An historical note on finite rotations, J. Appl. Mech., Vol. 56(1), pp. 139–145, 1989.
14. E. J. Haug, Computer Aided Kinematics and Dynamics of Mechanical Systems: Vol. 1, Basic Methods, Allyn and Bacon, 1989.
15. D. H. Sattinger, Group Theoretic Methods in Bifurcation Theory, Lecture Notes in Mathematics, Vol. 762, Springer-Verlag, Berlin, 1979.
16. J. M. T. Thompson and G. W. Hunt, A General Theory of Elastic Stability, Wiley, New York, 1973.
17. J. E. Marsden and S. R. Ratiu, Introduction to Mechanics and Symmetry, Texts in Applied Mathematics, Vol. 17, Springer-Verlag, New York; 2nd ed., 1999.
18. C. Meyer, Matrix Analysis and Applied Linear Algebra, SIAM, Philadelphia, 2000.
19. D. M. Bishop, Group Theory and Chemistry, Dover Publications, Oxford, 1973.
20. J. H. Ginsberg, Advanced Engineering Dynamics, Cambridge University Press, Cambridge, 1995.

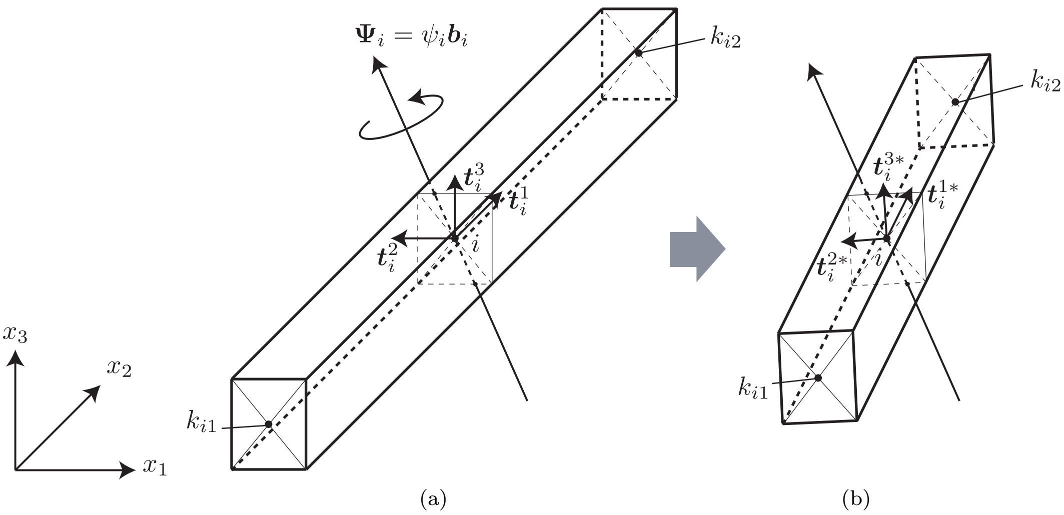

Fig. 13 Definition of global coordinates, unit vectors in local coordinates, and bar rotation; (a) before deformation, (b) after deformation

Appendix

A.1 Definition of incompatibility vector

Consider a bar element as shown in Fig. 13(a). We define the orthogonal reference frame of undeformed state using unit vectors as $(\boldsymbol{t}_i^1, \boldsymbol{t}_i^2, \boldsymbol{t}_i^3)$, where $\boldsymbol{t}_i^1$ is directed from the center of bar i to the second end node k_{i2}. Let $\boldsymbol{r}_{i1}$ and $\boldsymbol{r}_{i2}$ denote the vectors directing from the center of bar i to both ends connected to nodes k_{i1} and k_{i2}, respectively; i.e., $\boldsymbol{r}_{i1} = -(L_i/2)\boldsymbol{t}_i^1$ and $\boldsymbol{r}_{i2} = (L_i/2)\boldsymbol{t}_i^1$, where L_i is the length of bar i.

The rotation vector $\boldsymbol{\Theta}_k$ of node k is defined by the unit vector $\boldsymbol{n}_k$ of the axis of rotation and the angle θ_k as $\boldsymbol{\Theta}_k = \theta_k \boldsymbol{n}_k$. The rotation vector $\boldsymbol{\Psi}_i$ at the center of bar i is also defined by the unit vector $\boldsymbol{b}_i$ of the axis of rotation and the angle ψ_i as $\boldsymbol{\Psi}_i = \psi_i \boldsymbol{b}_i$. The reference frame $(\boldsymbol{t}_i^{1*}, \boldsymbol{t}_i^{2*}, \boldsymbol{t}_i^{3*})$ in deformed state is defined, as shown in Fig. 13(b), by rotating $(\boldsymbol{t}_i^1, \boldsymbol{t}_i^2, \boldsymbol{t}_i^3)$ around the axis $\boldsymbol{b}_i$ by the angle ψ_i as follows [13,14]:

$$\boldsymbol{t}_i^{l*} = \boldsymbol{b}_i(\boldsymbol{b}_i \cdot \boldsymbol{t}_i^l) + [\boldsymbol{t}_i^l - \boldsymbol{b}_i(\boldsymbol{b}_i \cdot \boldsymbol{t}_i^l)] \cos\psi_i - (\boldsymbol{t}_i^l \times \boldsymbol{b}_i) \sin\psi_i. \tag{A1}$$

The vectors $\boldsymbol{r}_{i1}^*$ and $\boldsymbol{r}_{i2}^*$ are defined similarly by rotating $\boldsymbol{r}_{i1}$ and $\boldsymbol{r}_{i2}$, respectively, along the axis $\boldsymbol{b}_i$ by the angle ψ_i.

Let $\Delta\boldsymbol{U}_{i1}, \Delta\boldsymbol{U}_{i2} \in \mathbb{R}^3$ and $\Delta\boldsymbol{\Theta}_{i1}, \Delta\boldsymbol{\Theta}_{i2} \in \mathbb{R}^3$ denote the translational and rotational incompatibility vectors, respectively, at two ends of bar i. If the bars are rigidly connected to nodes, the compatibility conditions are given as [11]

$$\Delta\boldsymbol{U}_{ij} = \boldsymbol{U}_{k_{ij}} - (\boldsymbol{V}_i + \boldsymbol{r}_{ij}^*) + \boldsymbol{r}_{ij} = \boldsymbol{0}, \quad (j = 1, 2,\ i \in \mathcal{M},\ k_{ij} \in \mathcal{K}), \tag{A2a}$$

$$\Delta\boldsymbol{\Theta}_{ij} = \boldsymbol{\Theta}_{k_{ij}} - \boldsymbol{\Psi}_i = \boldsymbol{0}, \quad (j = 1, 2,\ i \in \mathcal{M},\ k_{ij} \in \mathcal{K}). \tag{A2b}$$

where $\mathcal{K}$ and $\mathcal{M}$ are the sets of indices of all nodes and bars, respectively.

Next, we add rotational degrees of freedom at bar-ends, where arbitrarily inclined hinges or universal joints are expected to exist [7,8]. First, we define the compatibility of the inclined hinge. Let $\boldsymbol{f}_{ij}$ denote the direction vector of the hinge between node k_{ij} and bar i. The direction vectors $\boldsymbol{f}_{ij}^n$ and $\boldsymbol{f}_{ij}^b$ after rotations of nodes and bars, respectively, are computed as

$$\begin{aligned} \boldsymbol{f}_{ij}^n = \boldsymbol{n}_{k_{ij}}(\boldsymbol{n}_{k_{ij}} \cdot \boldsymbol{f}_{ij}) + [\boldsymbol{f}_{ij} - \boldsymbol{n}_{k_{ij}}(\boldsymbol{n}_{k_{ij}} \cdot \boldsymbol{f}_{ij})] \cos\theta_{k_{ij}} \\ - (\boldsymbol{f}_{ij} \times \boldsymbol{n}_{k_{ij}}) \sin\theta_{k_{ij}}, \end{aligned} \tag{A3a}$$

$$\boldsymbol{f}_{ij}^b = \boldsymbol{b}_i(\boldsymbol{b}_i \cdot \boldsymbol{f}_{ij}) + [\boldsymbol{f}_{ij} - \boldsymbol{b}_i(\boldsymbol{b}_i \cdot \boldsymbol{f}_{ij})] \cos\psi_i - (\boldsymbol{f}_{ij} \times \boldsymbol{b}_i) \sin\psi_i. \tag{A3b}$$

The compatibility conditions are given as the collinearity of vectors $\boldsymbol{f}_{ij}^n$ and $\boldsymbol{f}_{ij}^b$, which is expressed using the vector product as $\boldsymbol{e}_{ij} = \boldsymbol{f}_{ij}^b \times \boldsymbol{f}_{ij}^n = \boldsymbol{0}$ [14, 20]. We use the independent two components of this equation as

$$\boldsymbol{e}_{ij}^{(2)} = \left[e_{ij}^1, e_{ij}^2\right]^\top = \boldsymbol{0}. \tag{A4}$$

The condition (A2b) is to be replaced by (A4) if a hinge exists at the jth end of bar i, which means that number of constraints is reduced by one, when a hinge is placed at a bar end.

Next, we define the compatibility of a universal joint. If the jth end of bar i has a universal joint with orthogonal two axes $\boldsymbol{f}_{ij}^1$ and $\boldsymbol{f}_{ij}^2$, the equation to replace the condition of rotational incompatibility in $\boldsymbol{C}(\boldsymbol{W})$ is calculated as follows:

$$e_{ij}^{(1)} = \boldsymbol{f}_{ij}^b \cdot \boldsymbol{f}_{ij}^n = 0, \tag{A5}$$

where

$$\begin{aligned} \boldsymbol{f}_{ij}^n = \boldsymbol{n}_{k_{ij}}(\boldsymbol{n}_{k_{ij}} \cdot \boldsymbol{f}_{ij}^2) + [\boldsymbol{f}_{ij}^2 - \boldsymbol{n}_{k_{ij}}(\boldsymbol{n}_{k_{ij}} \cdot \boldsymbol{f}_{ij}^2)] \cos\theta_{k_{ij}} \\ - (\boldsymbol{f}_{ij}^2 \times \boldsymbol{n}_{k_{ij}}) \sin\theta_{k_{ij}}, \end{aligned} \tag{A6a}$$

$$\boldsymbol{f}_{ij}^b = \boldsymbol{b}_i(\boldsymbol{b}_i \cdot \boldsymbol{f}_{ij}^1) + [\boldsymbol{f}_{ij}^1 - \boldsymbol{b}_i(\boldsymbol{b}_i \cdot \boldsymbol{f}_{ij}^1)] \cos\psi_i - (\boldsymbol{f}_{ij}^1 \times \boldsymbol{b}_i) \sin\psi_i. \tag{A6b}$$

The compatibility equation (1) is an assemblage of (A2a), (A2b), (A4), (A5) and some support conditions. Here displacement vector $\boldsymbol{W}$ is composed of $\boldsymbol{U}, \boldsymbol{\Theta}, \boldsymbol{V}$ and $\boldsymbol{\Psi}$. Note that ψ_i and $\boldsymbol{b}_i$ are functions of $\boldsymbol{\Psi}$, and θ_k and $\boldsymbol{n}_k$ are functions of $\boldsymbol{\Theta}$.